

INFORMATION TO USERS

This manuscript has been reproduced from the microfilm master. UMI films the text directly from the original or copy submitted. Thus, some thesis and dissertation copies are in typewriter face, while others may be from any type of computer printer.

The quality of this reproduction is dependent upon the quality of the copy submitted. Broken or indistinct print, colored or poor quality illustrations and photographs, print bleedthrough, substandard margins, and improper alignment can adversely affect reproduction.

In the unlikely event that the author did not send UMI a complete manuscript and there are missing pages, these will be noted. Also, if unauthorized copyright material had to be removed, a note will indicate the deletion.

Oversize materials (e.g., maps, drawings, charts) are reproduced by sectioning the original, beginning at the upper left-hand corner and continuing from left to right in equal sections with small overlaps.

ProQuest Information and Learning
300 North Zeeb Road, Ann Arbor, MI 48106-1346 USA
800-521-0600

UMI[®]



Acoustic Noise Suppression for Speech Signals using Auditory Masking Effects

Joachim Thiemann



Department of Electrical & Computer Engineering
McGill University
Montreal, Canada

May 2001

A thesis submitted to the Faculty of Graduate Studies and Research in partial fulfillment
of the requirements for the degree of Master of Engineering.

© 2001 Joachim Thiemann



**National Library
of Canada**

**Acquisitions and
Bibliographic Services**

**395 Wellington Street
Ottawa ON K1A 0N4
Canada**

**Bibliothèque nationale
du Canada**

**Acquisitions et
services bibliographiques**

**395, rue Wellington
Ottawa ON K1A 0N4
Canada**

Your file Votre référence

Our file Notre référence

The author has granted a non-exclusive licence allowing the National Library of Canada to reproduce, loan, distribute or sell copies of this thesis in microform, paper or electronic formats.

The author retains ownership of the copyright in this thesis. Neither the thesis nor substantial extracts from it may be printed or otherwise reproduced without the author's permission.

L'auteur a accordé une licence non exclusive permettant à la Bibliothèque nationale du Canada de reproduire, prêter, distribuer ou vendre des copies de cette thèse sous la forme de microfiche/film, de reproduction sur papier ou sur format électronique.

L'auteur conserve la propriété du droit d'auteur qui protège cette thèse. Ni la thèse ni des extraits substantiels de celle-ci ne doivent être imprimés ou autrement reproduits sans son autorisation.

0-612-70255-3

Canada

Abstract

The process of suppressing acoustic noise in audio signals, and speech signals in particular, can be improved by exploiting the masking properties of the human hearing system. These masking properties, where strong sounds make weaker sounds inaudible, are calculated using auditory models. This thesis examines both traditional noise suppression algorithms and ones that incorporate an auditory model to achieve better performance. The different auditory models used by these algorithms are examined. A novel approach, based on a method to remove a specific type of noise from audio signals, is presented using a standardized auditory model. The proposed method is evaluated with respect to other noise suppression methods in the problem of speech enhancement. It is shown that this method performs well in suppressing noise in telephone-bandwidth speech, even at low Signal-to-Noise Ratios.

Sommaire

La suppression de bruit sonore présent dans les signaux audio, et plus particulièrement dans les signaux de parole, peut être améliorée en exploitant les propriétés de masque du système de perception sonore humain. Ces propriétés, où les sons plus intenses masquent les sons plus faibles, c'est-à-dire qui font que ces derniers deviennent inaudibles, sont calculées en utilisant un modèle de perception sonore. Ce mémoire étudie les algorithmes traditionnels de suppression de bruit et ceux qui incorporent un modèle de perception afin d'obtenir de meilleurs résultats. Une approche originale, qui utilise un modèle de perception standardisé, basée sur une méthode qui enlève du signal sonore un type de bruit particulier, est présentée. Cette nouvelle méthode est évaluée par rapport à d'autres méthodes de suppression de bruit pour les signaux de parole. Il est démontré que cette nouvelle approche donne de bons résultats pour la suppression de bruit dans des signaux de paroles, et ce, même à de bas niveaux de rapport signal à bruit.

Acknowledgments

This thesis would not have been possible without the encouragement and help from many people.

First and foremost, I would like to thank my thesis supervisor, Professor Peter Kabal. His guidance and support from the onset of this work was essential and key to its completion.

Thanks go out to all my friends at the Telecommunications and Signal Processing Lab, the McGill Outing Club, and my alma mater, Concordia. They all contributed directly or indirectly to this thesis, be it academic help, proofreading, volunteering to be a test subject, or just generally helping me to retain my sanity.

Finally, I wish to thank my parents for their love and unwavering support that made it all possible.

Contents

1	Introduction	1
1.1	Applications of Noise Suppression	1
1.2	General Noise Reduction Methods	3
1.2.1	Short-time Spectral Amplitude Methods	3
1.3	Auditory Models in Acoustic Noise Suppression	4
1.4	Previous Work	4
1.5	Thesis Contribution	5
1.6	Thesis Organization	5
2	Human Hearing and Auditory Masking	6
2.1	The Human Ear	6
2.1.1	The Outer Ear	7
2.1.2	The Middle Ear	7
2.1.3	The Inner Ear	7
2.1.4	The Basilar Membrane and the Hair Cells	8
2.2	Masking	9
2.2.1	Threshold of Hearing	10
2.2.2	Masking Effects	10
2.2.3	Critical Bands and the Bark scale	11
2.2.4	Excitation Patterns and the Masking Threshold	13
2.3	Summary	14
3	Spectral Subtraction	15
3.1	Basic Spectral Subtraction	15
3.1.1	Time to Frequency Domain Conversion	17

3.1.2	Spectral Subtraction as a Filter	17
3.1.3	Influence of windows on spectral subtraction	18
3.1.4	Noise estimation techniques	19
3.1.5	The Role of Voice Activity Detectors	20
3.1.6	Artifacts and distortion introduced by Spectral Subtraction	21
3.2	Related and derived methods	23
3.2.1	The Wiener Filter	23
3.2.2	Maximum Likelihood Envelope Estimator	24
3.2.3	The Ephraim and Malah Noise Suppressor	24
3.2.4	Filter Smoothing	25
3.2.5	Signal Subspace methods	26
3.2.6	Implementation of EVRC noise reduction	27
3.3	Comparison of Methods	29
3.4	Summary	31
4	Using Masking Properties in Spectral Subtraction Algorithms	33
4.1	Masking Models	34
4.1.1	The Johnston Model	34
4.1.2	The Perceptual Audio Quality Measure	37
4.1.3	Soulodre's Model	38
4.1.4	Perceptual Evaluation of Audio Quality	40
4.2	Perceptual based noise reduction	44
4.2.1	Tsoukalas' method for Speech Enhancement	45
4.2.2	Musical Noise Suppression	46
4.2.3	Virag's method	46
4.2.4	Tsoukalas' method for Audio Signal Enhancement	47
4.2.5	Soulodre's method	47
4.3	Using the PEAQ model in noise reduction	48
4.3.1	Choice of Masking Model	49
4.3.2	PNRF Implementation	49
4.3.3	Implementation Issues	50
4.3.4	Parameters and Modifications	50
4.4	Summary	52

5	Results	53
5.1	Test data	53
5.2	Objective Comparisons	54
5.3	Subjective Comparisons	58
5.4	Summary	61
6	Conclusion	62
6.1	Summary	62
6.2	Future Research Directions	63
6.2.1	Iterative clean speech estimation	64
6.2.2	Soft-decision VAD	64
6.2.3	Application to wide-band signals	64
6.2.4	Lower complexity masking model	65
A	Frequency bands for PEAQ	66
B	Subjective testing results	71
	References	73

List of Figures

1.1	Basic overview of an acoustic noise suppression system.	2
2.1	Structure of the human ear	6
2.2	Cross-section of the cochlea	8
2.3	Threshold of hearing in quiet	11
2.4	Masking curves for 1 kHz masking tone	12
2.5	Power spectrum, excitation pattern and masking threshold in perceptual domain	14
3.1	Basic structure of spectral subtraction systems	15
3.2	Bartlett and Hanning windows	19
3.3	Different noise estimation results	21
3.4	30 frames of Musical Noise in frequency domain	22
3.5	Origins of Musical Noise	23
3.6	EVRC Noise suppression structure	27
3.7	Gain curves of spectral subtraction algorithms	30
3.8	Gain curves of selected other methods	31
4.1	Incorporating a perceptual model in a spectral subtraction algorithm	44
4.2	Implementation of PNRF Gain Function	50
5.1	Setup for obtaining SNR, SNR _{SEG} , and SNR _{IMPR}	56

List of Tables

5.1	Objective measurement results with 0 dB initial SNR	57
5.2	Objective measurement results with 6 dB initial SNR	57
5.3	Subjective results for speech segments at 0 dB SNR	59
5.4	Subjective results for speech segments at 6 dB SNR	60
B.1	Number of answers indicating preference of "A" at 0 dB initial SNR	71
B.2	Number of answers indicating preference of "B" at 0 dB initial SNR	71
B.3	Number of answers indicating preference of "A" at 6 dB initial SNR	72
B.4	Number of answers indicating preference of "B" at 6 dB initial SNR	72

Chapter 1

Introduction

When a sound is picked up by a microphone, noise — in the sense of sounds other than the one of interest — will be picked up as well. It should be noted however, that in the context of acoustic signals, the definition of noise is a subjective matter. For example, the sounds made by the audience in a concert hall is usually considered to be part of the performance. It carries information about the audience reaction to the performance.

Usually, acoustic noise that was picked up by a microphone is undesirable, especially if it reduces the perceived quality or intelligibility of the recording or transmission. The problem of effective removal or reduction of noise (referred to here as *Acoustic Noise Suppression*, or ANS¹) is an active area of research, and is the topic of this thesis.

1.1 Applications of Noise Suppression

In the general sense, noise suppression has applications in virtually all fields of communications (channel equalization, radar signal processing, etc.) and other fields (pattern analysis, data forecasting, etc.) [1].

- *Telecommunications*

Perhaps the most common application of ANS is in the removal or reduction of background acoustic noise in telephone or radio communications. Examples of the former would be the hands-free operation of a cellular telephone in a moving vehicle.

¹A distinction must be made between *acoustic* noise suppression and *audible* noise suppression. Audible noise suppression is discussed in Ch. 4.

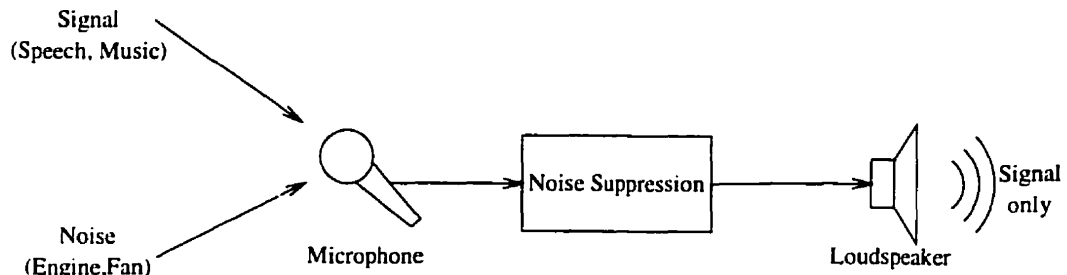


Fig. 1.1 Basic overview of an acoustic noise suppression system.

or a telephone on a factory floor. Examples of the latter would be communication in civil aviation and most military communications.

In these applications, generally the purpose of ANS is to improve the intelligibility of the speech signal, or at least to reduce listener fatigue. It is important to note in this context that — while undesirable — distortion of the original speech is tolerable if intelligibility is not affected.

Furthermore, in these types of applications, delays in the signal must be kept small. This places constraints on both algorithmic delays and computing complexity.

- *Audio Archive Restoration*

The restoration of sounds recorded on audio carriers (vinyl records, magnetic tape, etc.) has been a field of growing importance with the introduction of digital signal processing (DSP) methods. Unlike the applications mentioned above, processing delays are not an issue, but distortion of the original signal must be avoided [2].

While the carrier noise (such as tape hiss or phonograph crackle) is not strictly environmental acoustic noise, it may be treated as such since it is acoustic noise picked up with the intended signal by the same mechanism, either the needle of a record player or the magnetic head of a tape player.

Generally, the Signal-to-Noise Ratio (SNR) is much higher in Audio Archive Restoration than is the case for telecommunication applications.

These two application areas are merely given as examples, and there may in fact be considerable overlap. For example, a speech recording made under adverse conditions

may have a low SNR and allow for distortion, but the enhancement process will lack the complexity constraints. It is therefore desirable to have a method that works well in either application.

1.2 General Noise Reduction Methods

There are many ways to classify noise suppression algorithms. They may be single- or multi-sensor. In the latter, the spatial properties of the signal and noise sources can be taken into account. For example, beam-forming using a microphone array emphasizes sounds from a particular direction [1]. Another example is *adaptive noise cancellation* (ANC), which is a two-channel approach based on the primary channel consisting of signal and noise, and the secondary channel consisting of only the noise. The noise in the secondary channel must be correlated with the noise in the primary channel [3]. In the case of *adaptive echo cancellation* (AEC), the primary channel is the near-end handset, which contains the near-end signal and the reflection of the far-end signal. The secondary channel is the line from the far-end handset.

Some noise suppression methods try to exploit the underlying production method of the signal or the noise. In speech enhancement, this is usually done by linear prediction of the speech signal [3]. In audio enhancement, since the signal is too general to be modeled, the noise is modeled instead [2, 4].

1.2.1 Short-time Spectral Amplitude Methods

The noise suppression method discussed in this thesis is a single channel method based on converting successive short segments of speech into the frequency domain. In the frequency domain, the noise is removed by adjusting the discrete frequency “bins” on a frame-by-frame basis, usually by reducing the amplitude based on an estimate of the noise. The various methods (differentiated by the suppression rule, noise estimate and other details) are collectively known as Short-Time Spectral Amplitude (STSA), Spectral Weighting, or Spectral Subtraction methods.

1.3 Auditory Models in Acoustic Noise Suppression

In the above sections, only properties of the source of the signal and noise were exploited in the process of noise suppression. To further improve the performance of *acoustic* noise suppression (ANS) algorithms, properties of the human ear can be taken advantage of.

Research into human auditory properties is an ongoing process. However, available models of the human auditory system have been successfully used to improve the performance of speech and audio coding algorithms [5]. In these coding algorithms, the purpose is to take only as much of the signal as is perceptually relevant. This reduction of information allows the signal to be stored or transmitted using fewer bits.

Acoustic noise suppression methods incorporating these same perceptual models have shown significant gains in performance [4]. However, there is still room for improvements, and research into new methods continues.

1.4 Previous Work

Much of the work presented in this thesis is based on the work by Soulodre [4], where ANS methods were evaluated for the specific problem of removing camera noise from film soundtracks. Soulodre examined the properties of camera noise (generated mainly by the lens shutter) in detail, and presented a novel auditory model and an ANS method. Using a combination of frame synchronization, sub-band processing and a novel auditory model, Soulodre achieved noise removal at a Signal-to-Noise Ratio of up to 12 dB lower than required by traditional noise reduction methods, with little or no audible distortion of the signal.

Also, auditory-based ANS methods were developed by Tsoukalas *et al*, who in [6] used an iterative approach to remove audible noise from speech signals. This method aggressively removes all but the most audible components of the signal, resulting in almost complete noise removal at the expense of some signal distortion. In [7], a method for reduction of noise in audio signals is presented, based on calculating an auditory model of the noise and removing it from an auditory model of the noisy signal.

In yet another approach, Virag [8] uses an auditory model to adjust the parameters of a non-auditory noise suppression procedure to improve its performance and reduce artifacts.

Haulick *et al* [9] used a more direct approach, using the auditory masking threshold

in an attempt to identify and then suppress musical noise (a common artifact of noise reduction algorithms).

1.5 Thesis Contribution

This thesis presents an overview of noise suppression using auditory models. Some of the existing auditory models and suppression rules are presented. The presented auditory masking based suppression methods are implemented using the most recent and best-defined auditory model. A new method based on the generalization of the method from Soulodre [4], is presented as a viable speech and audio enhancement method. This method is compared objectively and subjectively with the implementations of the other methods. Results show that the new method achieves a good combination of low residual noise, low signal distortion, and low complexity.

1.6 Thesis Organization

The fundamentals of human hearing and the mechanics of the ear are explained in Chapter 2. The concepts of masking and the threshold of hearing are introduced. Chapter 3 introduces algorithms to suppress noise using STSA methods that do not incorporate auditory effects. In Chapter 4, some of the mathematical models of the hearing system are presented, and noise suppression algorithms that incorporate those models. A standard auditory model is incorporated into adapted versions of the ANS algorithms. The results of comparing the various methods are presented in Chapter 5. Chapter 6 summarizes and concludes the thesis.

Chapter 2

Human Hearing and Auditory Masking

2.1 The Human Ear

The human auditory system consists of the ear, auditory nerve fibers, and a section of the brain. It converts sound waves into sensations perceived by the auditory cortex.

The ear is the outer peripheral system which converts acoustic energy (sound waves) into electrical impulses that are picked up by the auditory nerve. The ear itself is divided into three parts, the outer, middle, and inner ear, as shown in Fig. 2.1.

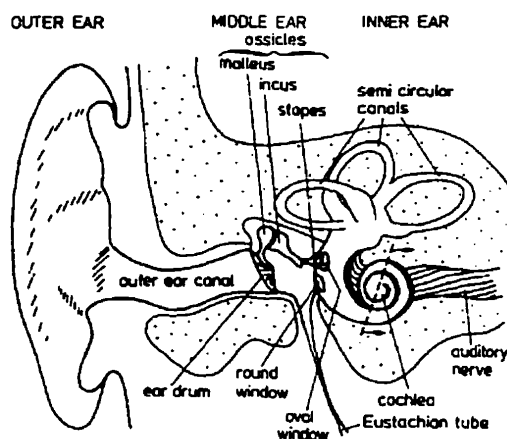


Fig. 2.1 Structure of the human ear [10]

2.1.1 The Outer Ear

The outer ear consists of the *pinna* (the visible part of the ear), the *meatus* (ear canal), and terminates at the *tympanic membrane* (eardrum). The pinna collects sounds and aids in sound localization, that is to be more sensitive to sounds coming from the front of the listener [11].

The meatus is a tube which directs the sound to the tympanic membrane. A cavity with one end open and the other closed by the tympanic membrane, the meatus acts as a quarter-wave resonator with a center frequency around 3000 Hz. This particular structure likely aids in the perception of obstruents¹, which have much of their energy content in this frequency region.

2.1.2 The Middle Ear

The middle ear is considered to begin at the tympanic membrane and contains the *ossicles*, a set of three small bones. These bones are named *malleus* (hammer), *incus* (anvil), and *stapes* (stirrup). Acting primarily as levers performing an impedance matching transformation (from the air outside the eardrum to the fluid in the cochlea), they also protect against very strong sounds. The *acoustic reflex* activates middle ear muscles, to change the type of motion of the ossicles when low-frequency sounds with SPL above 85–90 dB reach the eardrum. Attenuating pressure transmission by up to 20 dB, the acoustic reflex is also activated during voicing in the speaker's own vocal tract [11]. Due to their mass, the ossicles act as a low-pass filter with a cutoff frequency around 1000 Hz.

2.1.3 The Inner Ear

The inner ear is a bony structure comprised of the semicircular canals of the vestibula and the cochlea. The vestibula is the organ that helps balancing the body and has no apparent role in the hearing process [12]. The cochlea is a cone-shaped spiral in which the auditory nerve terminates. It is the most complex part of the ear, wherein the mechanical pressure waves are converted into electrical pulses.

The cochlea is a tapered tube filled with a gelatinous fluid (*endolymph*). At its base this tube has a cross section of about 4 mm², and two membrane covered openings, the

¹Sounds produced by obstructing the air flow in the vocal tract, such as /s/ and /t/.

Oval Window and the Round Window. The Oval Window is connected to the ossicles. The Round Window is free to move to equalize the pressure since the endolymph is incompressible.

The cochlea has two membranes running along its length, the Basilar Membrane (BM) and Reissner's Membrane. These two membranes divide the cochlea into three channels, as seen in Fig. 2.2.

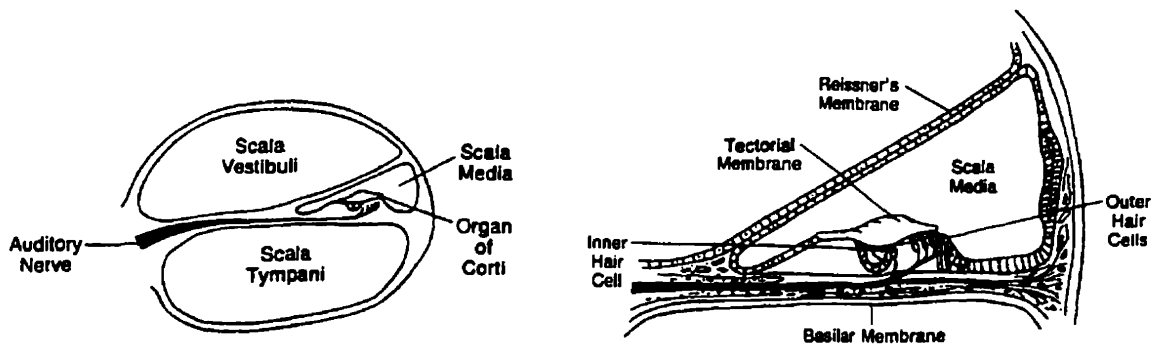


Fig. 2.2 Cross-section of the cochlea [11]

These channels are called the Scala Vestibuli, the Scala Media, and the Scala Tympani. Pressure waves travel from the Oval window through the Scala Vestibuli to the apex of the cochlea. A small opening (*helicotrema*) connects the Scala Vestibuli to the Scala Tympani. The sound pressure waves then travel back to the base through the Scala Tympani, terminating at the Round Window. Since the velocity of sound in the cochlea is about 1600 m/s, there is no appreciable phase delay.

2.1.4 The Basilar Membrane and the Hair Cells

The mechanics of the Basilar Membrane (BM) can explain many effects of masking (described below). Within the BM, mechanical movements are transformed into nerve stimuli transmitted to the brain. The BM performs a crucial part of sound perception. It is narrow and stiff at the base of the cochlea, gradually tapering to a wide and pliable end at the apex of the cochlea. Each point on the cochlea can be viewed as a mass-spring system with a resonant frequency that decreases from base to apex. A frequency to place transformation is performed, such that if a pure tone is applied to the Oval Window, a section of the

BM will vibrate. The amplitude of BM vibration is dependent on distance from the oval window and the frequency of the stimulus. The BM vertical displacement is small near the oval window. Growing slowly, the vertical displacement reaches a maximum at a certain distance from the oval window. The amplitude of the vertical displacement then rapidly dies out in the direction of the helicotrema. The frequency of a signal that causes maximum displacement at a given point of the BM is called the Characteristic Frequency (CF).

The vibration of the BM is picked up by the hair cells of the Organ of Corti. There are two classes of hair cells, the Inner Hair Cells (IHC) and Outer Hair Cells (OHC). About 90% of *afferent* (ascending) nerve fibers that carry information from the cochlea to the brain terminate at the IHC. Most of the *efferent* (descending) nerve fibers terminate at the OHC, which greatly outnumber the IHC. Empirical observations suggests that the OHC, with direct connection to the tectorial membrane, can change the vibration pattern of the BM, improving the frequency selectivity of the auditory system [12, 13].

Measurements from afferent auditory nerves have shown further nonlinearities in the auditory system. All IHC show a spontaneous rate of firings in the absence of stimuli. As a stimulus (such as a tone burst at the CF for the IHC) is applied, the neuron responds with a high rate of firings, which after approximately 20 ms decreases to a steady rate. Once the stimulus is removed, the rate falls below the spontaneous rate for a short time before returning to the spontaneous rate [12].

2.2 Masking

Human auditory masking is a highly complex process which is only partially understood, yet we experience the effects in everyday life. In noisy environments, such as an airport or a train station, noise seems to have a habit of lowering intelligibility just enough so that you miss the last call for the flight or train you have to catch.

The American Standards Association (ASA) defines masking as the process or the amount (customarily measured in decibels) "by which the threshold of audibility is raised by the presence of another (masking) sound" [13]. Simply put, one sound cannot be heard because of another (typically louder) sound being present.

2.2.1 Threshold of Hearing

In order to be audible, sounds require a minimum pressure. Due in part to filtering in the outer and middle ear, this minimum pressure (considering for now a pure tone) varies considerably with frequency. This threshold of hearing (audibility) is unique from person to person and furthermore changes with a person's age. Figure 2.3 shows the level of sound pressure above which 10%, 50%, and 90% of subjects 20 to 25 years of age can hear a test tone in quiet [10]. For signal processing purposes, the threshold is approximated by [14]

$$T_q(f) = 3.64(f/1000)^{-0.8} - 6.5e^{-0.6(f/1000-3.3)^2} + 10^{-3}(f/1000)^4 \text{ (dB SPL)}, \quad (2.1)$$

which is measured in dB SPL, or dB relative to 20 μ Pa [15]. This approximation is shown as a solid line in Fig. 2.3.

It is assumed that the threshold of audibility is a result of the internal noise of the auditory system. Effectively, the internal noise is masking a very weak external signal.

2.2.2 Masking Effects

In the most broad categories, masking effects can be classified as simultaneous or temporal. In simultaneous masking, the masking sound and the masked sound are present at the same time. Temporal masking refers to the effect of masking with a small time offset.

Due to the limited time resolution of the algorithm presented in the following chapters, temporal masking is of limited use, but can be used to hide preechoes². *Forward masking*, where a sound is inaudible for a short time after the masker has been removed, can be between 5 ms and more than 150 ms. *Backward masking*, where a weak signal is inaudible before the onset of the masking signal, is usually below 5 ms [16].

In masking, we need to consider two kinds of sounds that can act as the masker. Noise-like sounds with a broad spectrum and little or no phase coherence can mask sounds with levels as little as 2–6 dB below the masker. Tone-like sounds need to be much louder, needing as much as 18–24 dB higher amplitude to mask other tones or noise, partially due to phase distortion and the appearance of difference tones [10, 11].

Masking also is somewhat dependent of the absolute level of the masker. Fig. 2.4 shows the amount of masking provided by a 1 kHz tone at various absolute sound pressure levels

²Artifacts introduced by frame based signal processing algorithms. See the following chapter.

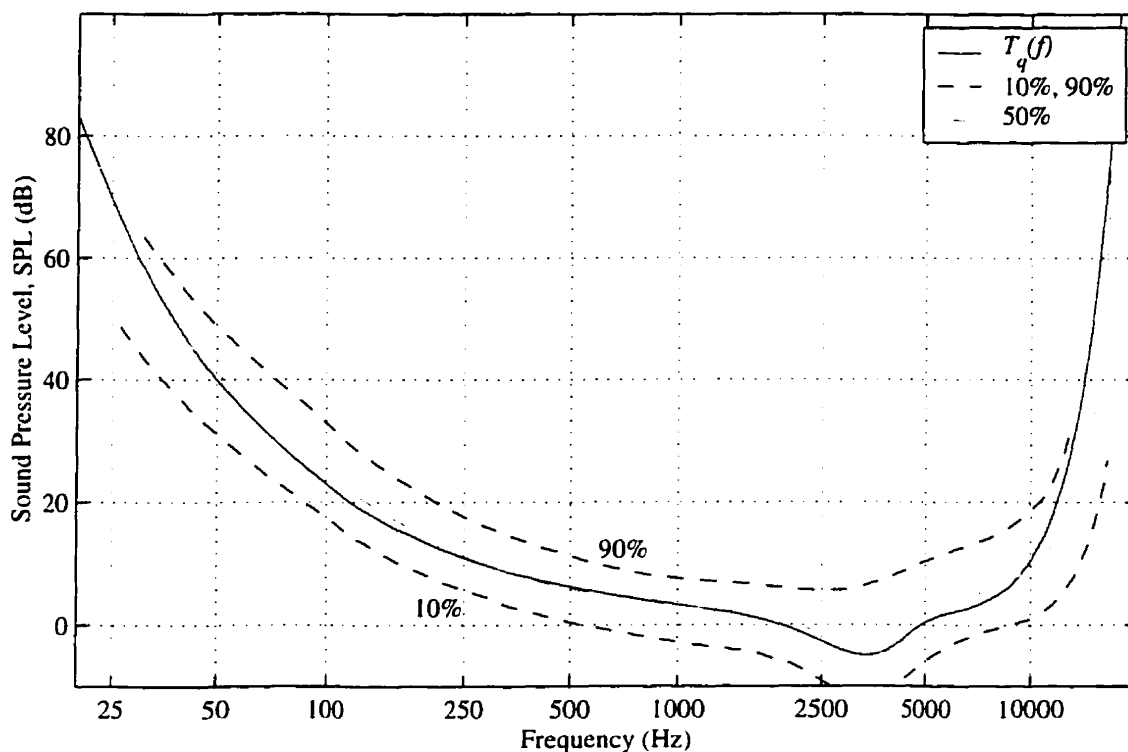


Fig. 2.3 Threshold of hearing in quiet, the SPL required such that 10%, 50% and 90% of subjects could detect a tone, empirical data from [10]. Also pictured is the approximation from (2.1) (solid line).

L_M . It can be seen that the slope of the upwards part of the masking curve varies with level.

It should be noted that these curves are only averages, and vary from person to person. To illustrate, the dotted lines in Fig. 2.4 show the masking provided by a 60 dB pure tone at 1 kHz for two persons at the extremes of the sample set.

2.2.3 Critical Bands and the Bark scale

The frequency selectivity of masking effects is described in terms of *Critical Bands* (CB). In general, a CB is the bandwidth around a center frequency which marks a (sudden) change in subjective response [15]. For example, the perceived loudness of narrowband noise of fixed power density is independent of bandwidth as long as the noise is confined within

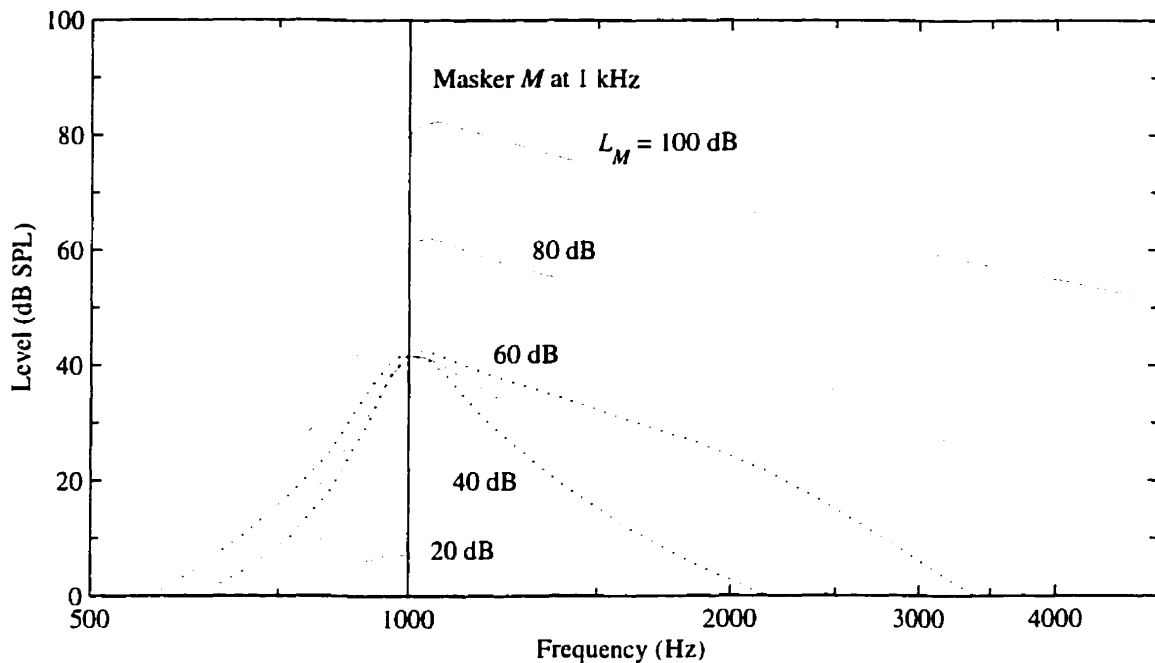


Fig. 2.4 Masking curves for 1 kHz masking tone, on a logarithmic frequency scale [10]

a CB. If the bandwidth of the noise is further increased, the perceived loudness will also increase.

While the exact mechanism behind this abrupt change in frequency selectivity is not known, at least some of it can be explained in Basilar Membrane (BM) and Inner Hair Cell (IHC) behavior. As discussed above, the BM is not a perfect frequency discriminator but each point on the BM responds to a range of frequencies. This behavior is modeled as a bank of overlapping bandpass filters, called *auditory filters*. The shape of these filters is not exactly known, and can change with signal level, hence they are not linear. However, this nonlinearity is usually ignored. A more important property of the auditory filters is that their bandwidth changes with frequency.

Moore [13] describes CB as a measure of the 'effective bandwidth' of the auditory filters, though it must be noted that the actual width of the CB is narrower than the corresponding auditory filter.

The actual width of Critical Bands is still in dispute. According to Zwicker [10] the

bandwidth of Critical Bands is relatively constant below 500 Hz, but above that increases approximately in proportion with frequency. Moore's measurements (to distinguish them from the traditional CB, called Effective Rectangular Band, ERB) indicated narrower bandwidths, and found changes in bandwidth even below 500 Hz. Both claim to correspond to fixed distances on the BM, 1.3 mm for Zwicker's CB and 0.9 mm Moore's ERB.

Aside from masking, the concept of auditory filtering and Critical Bands has many implications, and is the single most dominant concept in auditory theory [15]. Thus, an absolute frequency scale based on the original (as used by Zwicker) CB measurements is in common use. This scale is called the Bark scale, and the common function to convert from Hz to Bark is (from Zwicker [10, 17])

$$z(f) = 13 \arctan(0.00076f) + 3.5 \arctan \left[\left(\frac{f}{7500} \right)^2 \right], \quad (2.2)$$

and the bandwidth (in Hz) of a CB at any frequency is given by

$$BW_c(f) = 25 + 75 [1 + 1.4(f/1000)^2]^{0.69}. \quad (2.3)$$

The bandwidth in Bark of a CB at any frequency is (by definition) 1. This "normalization" of Critical Bands in frequency domain allows for simpler a calculation of auditory effects, such as the *spread of masking*, which is the amount of masking provided by signals outside the immediate critical band.

2.2.4 Excitation Patterns and the Masking Threshold

By modeling the auditory system as a filter bank, the excitation in dB at each point of the BM can be calculated. This *Excitation Pattern* is used in some algorithms as a first step to calculating the *Masking Threshold*, which indicates the threshold of hearing in the presence of a signal. However, there are many ways of calculating the excitation pattern. This is mostly due to differing models of auditory filters, from relatively crude non-overlapping rectangular filters to more complex shapes such as Roex(p) and Gammatone Filters [15]. Furthermore, there is still much dispute about how adjacent critical bands interact, both how excitations add up, or the shape of *spreading functions* which describe the spread of masking.

Some of the more common methods of modeling the excitation pattern and the masking

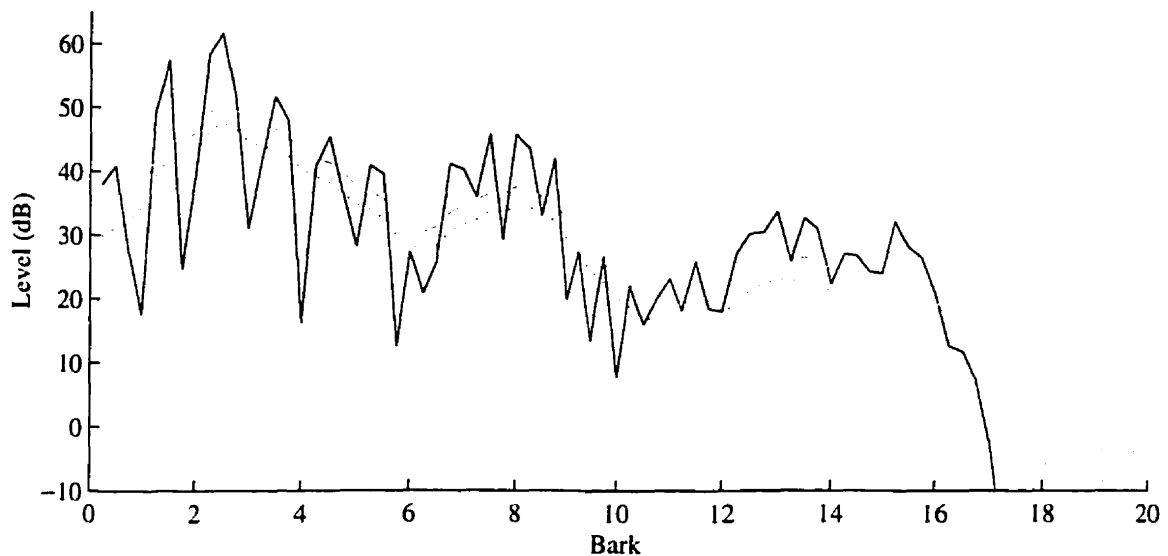


Fig. 2.5 Power spectrum (solid line), excitation pattern (dashed line) and masking threshold (dotted line) of a segment of speech, in perceptual domain.

threshold for a given signal are described in Chapter 4. Figure 2.5 shows a single frame of speech, transformed into the perceptual domain, with the resulting excitation pattern and masking thresholds, using the method described in Sec. 4.1.4. An overview and comparison of various methods was presented in [18].

2.3 Summary

This chapter describes the process of sound transmission from the outer ear to the cochlea, where the mechanical movement is converted into stimuli perceived by the brain. Masking is introduced and some masking effects described. The frequency resolution of the auditory system is described in terms of auditory filters and critical bands. The Bark scale is presented to allow modeling the frequency analysis performed by the basilar membrane.

Chapter 3

Spectral Subtraction

Spectral subtraction is a method to enhance the perceived quality of single channel speech signals in the presence of additive noise. It is assumed that the noise component is relatively stationary. Specifically, the spectrum of the noise component is estimated from the pauses that occur in normal human speech. Fig. 3.1 shows the simplified structure of basic spectral subtraction systems.

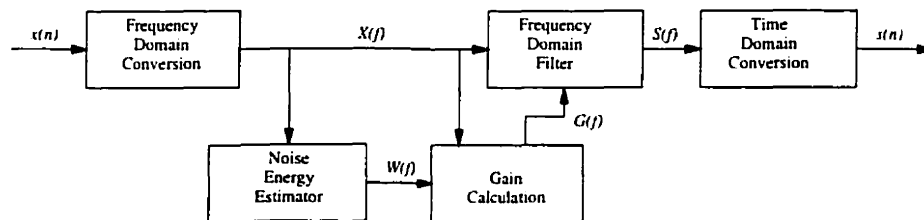


Fig. 3.1 Basic structure of spectral subtraction systems

The first detailed treatment of spectral subtraction was performed by Boll [19, 20]. Later papers [21, 22] expanded and generalized Boll's method to power subtraction, Wiener filtering and maximum likelihood envelope estimation.

3.1 Basic Spectral Subtraction

Speech which is "contaminated" by noise can be expressed as

$$x(n) = s(n) + v(n), \quad (3.1)$$

where $x(n)$ is the speech with noise, $s(n)$ is the “clean” speech signal and $v(n)$ is the noise process, all in the discrete time domain. What spectral subtraction attempts to do is to estimate $s(n)$ from $x(n)$. Since $v(n)$ is a random process, certain approximations and assumptions must be made. One approximation is that the noise is (within the time duration of speech segments) a short-time stationary process. Specifically, it is assumed that the power spectrum of the noise remains constant within the time duration of several speech segments (typically words or sentence fragments). Also, noise is assumed to be uncorrelated to the speech signal. This is an important assumption since, as explained in Sec. 3.1.4 below, the noise is estimated from pauses in the speech signal. Finally, it is assumed that the human ear is fairly insensitive to phase, such that the effect of noise on the phase of $s + v$ can be ignored.

If the noise process is represented by its power spectrum estimate $|\hat{W}(f)|^2$, the power spectrum of the speech estimate $|\hat{S}(f)|^2$ can be written as

$$|\hat{S}(f)|^2 = |X(f)|^2 - |\hat{W}(f)|^2, \quad (3.2)$$

since the power spectrum of two uncorrelated signals is additive. By generalizing the exponent from 2 to a , Eq. (3.2) becomes

$$|\hat{S}(f)|^a = |X(f)|^a - |\hat{W}(f)|^a. \quad (3.3)$$

This generalization is useful for writing the filter equation (3.6) below [1, 22].

The speech phase $\phi_{\hat{S}}(f)$ is estimated directly from the noisy signal phase $\phi_X(f)$.

$$\phi_{\hat{S}}(f) = \phi_X(f) \quad (3.4)$$

Thus a general form of the estimated speech in frequency domain can be written as

$$\hat{S}(f) = \left(\max(|X(f)|^a - k|\hat{W}(f)|^a, 0) \right)^{\frac{1}{a}} \cdot e^{j\phi_X(f)}, \quad (3.5)$$

where $k > 1$ is used to *overestimate* the noise to account for the variance in the noise estimate, as explained below. The inner term $|X(f)|^a - k|\hat{W}(f)|^a$ is limited to positive values, since it is possible for the overestimated noise to be greater than the current signal.

3.1.1 Time to Frequency Domain Conversion

The statistical properties of a speech signal change over time, specifically, from one phoneme to the next. Within phonemes, which average about 80 ms in duration [11], the statistics of the signal are relatively constant. For this reason, the processing of speech signals is typically done in short time sections called frames. The size of frames is typically 5 to 50 ms [1], though rarely larger than 32 ms. In these short-time segments, speech can be considered stationary [19, 22, 23]. The frames of time domain data are windowed (the effects of the window employed are discussed in Section 3.1.3 below) and then converted to frequency domain using the Discrete Fourier Transform (DFT). To indicate discrete frequency domain, the notation $X(m, p) \triangleq X(m \frac{f_s}{M})$, where $2M$ is the order of the DFT and p is the frame index, is used. The frame index p is also dropped if the operation is local in time (that is, if the operation is *memoryless*, and not directly using data from previous time frames).

Generally, when dealing with speech signals, the signal operated on is assumed to be sampled at $f_s = 8000$ Hz. However, until auditory effects are considered, the sampling rate is irrelevant, as long as the length of frames is kept appropriate as mentioned in the previous paragraph. It should be noted that the effective frequency resolution depends only on the framesize.

3.1.2 Spectral Subtraction as a Filter

It is convenient to think of the spectral subtraction as a filter, denoted here by $G(m, p)$, which operates on the received signal. Specifically, the filter is implemented in the frequency domain by

$$\begin{aligned} \hat{S}(m) &= X(m)G(m) \\ &= X(m) \left(\max \left(\frac{|X(m)|^a - k|\hat{W}(m)|^a}{|X(m)|^a}, 0 \right) \right)^{\frac{1}{a}} \\ &= X(m) \left(\max \left(1 - k \frac{|\hat{W}(m)|^a}{|X(m)|^a}, 0 \right) \right)^{\frac{1}{a}}, \quad m = 0, \dots, M-1. \end{aligned} \quad (3.6)$$

Equation (3.6) is the conventional spectral subtraction equation. It should be noted that it is possible for $1 - k \frac{|\hat{W}(m)|^a}{|X(m)|^a}$ to be less than 0. In this case, $G(m)$ is set to 0 at those

frequencies, or to some small positive value α , to create a “noise floor.” Using a noise floor, first proposed by Berouti *et al* [24], has been found to reduce artifacts such as musical noise [2]. The generalized formula for the zero-phase filter in the frequency domain is given by Eq. (3.7).

$$G(m) = \max \left\{ \left(\max \left(1 - k \frac{|\hat{W}(m)|^a}{|X(m)|^a}, 0 \right) \right)^{\frac{1}{a}}, \alpha \right\}, \quad m = 0, \dots, M - 1. \quad (3.7)$$

Varying the parameters k , a and α is used to achieve tradeoffs between residual noise and distortion in the speech signal. The factor k controls the amount of subtraction, based on the overestimation of the noise mentioned above. Typically, a value of 1.5 is used, though Berouti *et al* suggested values in the range of 3 to 5 when proposing this method [24]. Typical values of a are 1 for magnitude spectral subtraction (as used by Boll [19]) and 2 for power spectral subtraction (as used by McAulay and Malpass [21]), though other values may be used.

3.1.3 Influence of windows on spectral subtraction

Any signal processing done via manipulation of the short-time spectra requires transforming the time-domain signal to the frequency domain [25]. The spectra can then be modified, and finally transformed back to the time domain. To avoid discontinuities at the frame boundaries, the frames overlap, so the segment actually being processed is longer than a frame. Boll [19] used 50% overlap, meaning that if the framesize is 128 samples long (16 ms), in each iteration 256 samples (32 ms) would be processed.

Since some (or, in the case of 50% overlap, all) samples get processed twice, the frames are windowed. There is one necessary condition for proper reconstruction, which is that the windows will add to unity. Oppenheim and Lim used the equation

$$\sum_m w(n + mF) = 1. \quad \text{for all } n, \quad (3.8)$$

where F is the frame length. Only an analysis window was used by Oppenheim and Lim, implying a rectangular synthesis window. Other analysis/synthesis window combinations

can provide improved performance [4]. Eq. (3.8) then becomes

$$\sum_m w_a(n + mF)w_s(n + mF) = 1, \quad \text{for all } n, \quad (3.9)$$

where w_a and w_s represent the analysis and synthesis windows, respectively. It is convenient to have the same analysis and synthesis window, thus $w_a(n) = w_s(n) = \sqrt{w(n)}$. Two possible choices for $w(n)$ are the Bartlett (triangular) and Hanning (\sin^2) window, shown in Fig. 3.2.

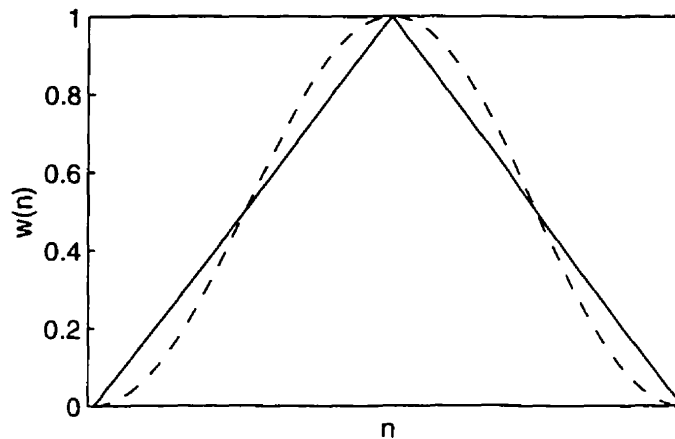


Fig. 3.2 Bartlett (solid) and Hanning (dashed) windows

The shape of the window has some effect on the frequency domain representation [26, 27], but Oppenheim and Lim [22] suggest that the shape has little effect on the performance of short-time spectral amplitude (STSA) based speech enhancement algorithms. However, when an auditory model is used, the window does become important [4, 5].

3.1.4 Noise estimation techniques

The spectrum of the noise during speech periods is not exactly known. However, it can be estimated, since (as mentioned above) the noise is assumed to be a short-time stationary process. The estimate of the noise is taken from the speech pauses which are identified using a voice activity detector (see below). The estimate of the noise spectrum using a finite length DFT is referred to as a *periodogram* [1, 26]. If a non-rectangular window is

used, the estimator is called a *modified periodogram* [27]. This modified periodogram can be obtained from the analysis section of the spectral subtraction algorithm.

To reduce the variance of the noise estimate, the Welch method of averaging modified periodograms can be used. The standard Welch method uses a fixed number of periodograms averaged with equal weights. As an alternative, an exponential average can be used, which can be efficiently implemented and thus is used almost exclusively in actual implementations of noise suppression algorithms. The noise power spectrum estimate $|\hat{W}(m, p)|^2$ is updated from the power spectrum of the current frame ($|X(m, p)|^2$) *if the current frame is considered to be noise only* by

$$|\hat{W}(m, p)|^2 = \lambda_N |\hat{W}(m, p-1)|^2 + (1 - \lambda_N) |X(m, p)|^2, \quad m = 0, \dots, M-1, \quad (3.10)$$

where λ_N is the noise forgetting factor. The value of λ_N determines a tradeoff between the variance of $|\hat{W}(m, p)|^2$ (or accuracy of the noise spectrum estimate) and responsiveness to changing noise conditions. A typical value of λ_N for 20 ms frames is 0.9 [1], resulting in a time constant of about 10 frames, or 200 ms.

Fig. 3.3 shows the noise estimates for white noise obtained from different methods. The framesize was chosen to be 64 samples, and the overlap between frames 50%. The solid line shows the noise estimate by exponential averaging, $\lambda_N = 0.9$. The other lines show the estimate by the Welch method of averaging modified periodograms. The dashed and the dotted lines were obtained by averaging 10 and 100 frames respectively. Note that the Exponential Average method produces an estimate that is better than the Welch method at 10 frames, yet implementing the former requires less memory and is less computationally intensive.

3.1.5 The Role of Voice Activity Detectors

In a practical setting, the voice activity detector (VAD) plays a very important role in the noise estimation. In general, it is preferable to have a VAD which errs on the side of misclassifying noise as speech. A VAD falsely classifying speech as noise can cause the system to erroneously remove speech components.

The design of a VAD is nontrivial. In one modern implementation of a speech codec, specifically the Enhanced Variable Rate Coder (EVRC) [28], the VAD is an integral part of the noise suppressor, which is described in Sec. 3.2.6 below. To detect speech presence,

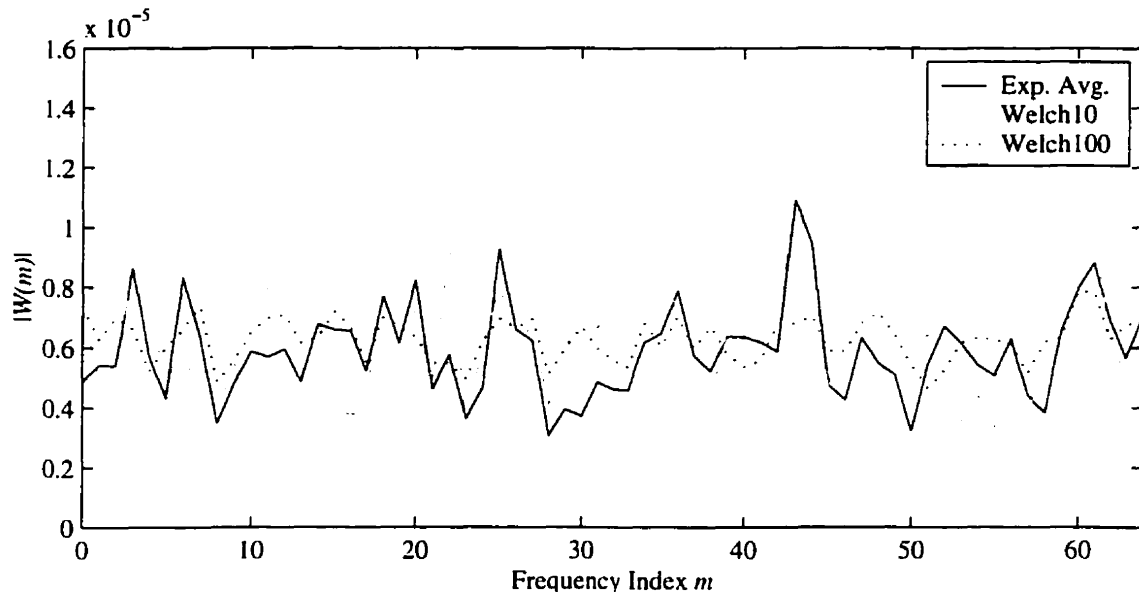


Fig. 3.3 Different noise estimation results. Solid line: Exponential average, dashed line: Welch Periodogram, 10 frames, dotted line: Welch Periodogram, 100 frames.

a comparison of the current signal energy to the current noise estimate is performed, along with rules based on temporal speech statistics. It should be noted that the VAD for Adaptive Multi-Rate (AMR) GSM coder (06.94 version 7.1.0) uses a very similar scheme [29].

The problem of reliable detection of speech in noise is beyond the scope of this thesis. However, the influence of the VAD on the performance must be taken into account during evaluation of noise suppression algorithms.

3.1.6 Artifacts and distortion introduced by Spectral Subtraction

Unfortunately, using spectral subtraction techniques introduces artifacts which can be very annoying to listeners since the distortions sound very unnatural.

One of the artifacts is phase distortion, caused by the assumption that the ear is insensitive to the phase. The phase is taken from the noisy signal, as shown by Equation (3.4). Experiments with “ideal” spectral subtraction (where the magnitude of each frame is taken from the clean signal and the phase from the noisy signal) show that this becomes significant as the SNR approaches 0 dB, resulting in a “hoarse” sounding voice.

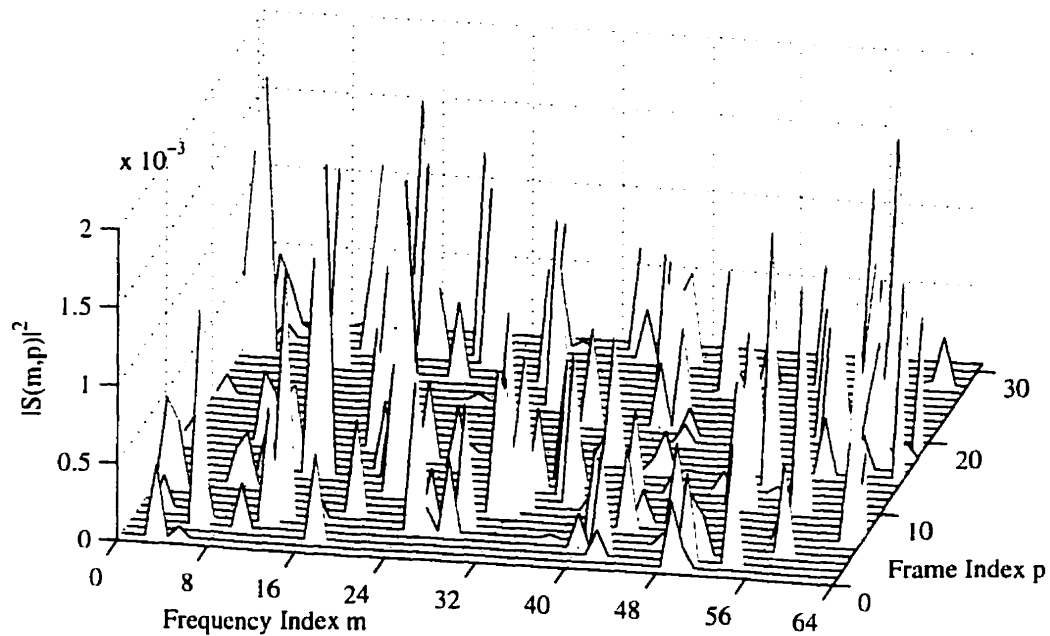


Fig. 3.4 30 frames of Musical Noise in frequency domain

Another artifact is caused by the processing in the frequency domain, using short-time spectra. Multiplying two DFTs results in circular convolution in the time domain [26]. If the frames are long, this “temporal smearing” is audible as pre- and postechos, but in shorter frames merely as noise that is correlated with the signal. Using a maximum overlap between frames (50%) and a smooth (non-rectangular) synthesis window can greatly reduce these echos.

The most noticeable (and most disturbing) artifact introduced by standard spectral subtraction algorithms is known as musical noise, caused by the variance in the magnitude of short-time spectra of random signals. Musical Noise is a result of the frame-based approach to noise reduction. It consists of short (the length of a frame) isolated tone bursts, which are distributed randomly across frequency. Musical Noise sounds very unnatural and is therefore highly disturbing to the listener.

Figure 3.4 shows musical noise generated by processing a signal consisting of white noise. The signal was processed by power spectral subtraction with $k = 1.5$. Figure 3.5 illustrates the origins of musical noise more clearly by examining a single frame. The solid line shows the current noise estimate $|\hat{W}(m)|^2$, multiplied by k . The dotted line shows

the power spectrum of the current input frame, $|X(m)|^2$. The magnitude spectrum of the resulting clean signal estimate $|\hat{S}(m)| = |X(m)G(m)|$ is shown as a dashed line.

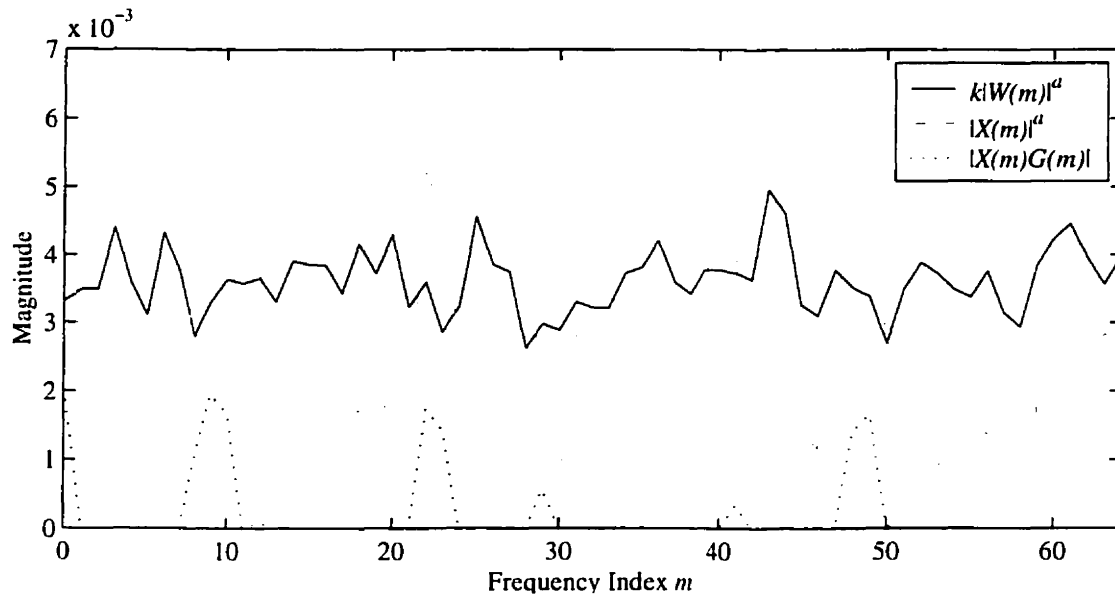


Fig. 3.5 Origins of Musical Noise

Since the development of STSA subtractive algorithms, much effort has been concentrated in reducing or eliminating Musical Noise.

3.2 Related and derived methods

Since the development of the Spectral Subtraction method by Boll [19], the basic problem has been attacked by changing the basic assumptions, in particular about the spectral magnitude of the noisy signal. Changing the basic assumption of (3.2) results in a different gain rule. For reference, some methods are presented here.

3.2.1 The Wiener Filter

Derived in a similar manner as the power spectral subtraction method, the Wiener Filter attempts to minimize the mean-squared error in frequency domain [21, 22]. Writing $\mathcal{R}(m, p)$ for the signal-to-noise ratio (SNR) of the m^{th} frequency bin, the generally cited form of

the Wiener filter is Eq. (3.11).

$$G_W(m) = \frac{\mathcal{R}(m)}{\mathcal{R}(m) + 1} \quad (3.11)$$

To compare (3.7) and (3.11), $\mathcal{R}(m)$ is given as

$$\mathcal{R}(m) = \begin{cases} \frac{|X(m)|^2 - |\hat{W}(m)|^2}{|\hat{W}(m)|^2}, & |X(m)|^2 > |\hat{W}(m)|^2 \\ 0 & \text{otherwise,} \end{cases} \quad (3.12)$$

and substituting in Eq. (3.11), we get

$$G_W(m) = \begin{cases} 1 - \frac{|\hat{W}(m)|^2}{|X(m)|^2}, & |X(m)|^2 > |\hat{W}(m)|^2, \\ 0 & \text{otherwise,} \end{cases} \quad (3.13)$$

where the similarity to Eq. (3.7) is obvious. In fact, $G_W(m) = \sqrt{G(m)}$ with $k = 1$, $a = 2$, and $\alpha = 0$.

3.2.2 Maximum Likelihood Envelope Estimator

The Maximum Likelihood Envelope Estimator (MLEE) is based on the assumption that the speech signal is characterized by a deterministic waveform of unknown amplitude and phase [21]. The MLEE is characterized by its gain function

$$G_{\text{MLEE}} = \left[\frac{1}{2} + \frac{1}{2} \sqrt{1 - \frac{|\hat{W}(m)|^2}{|X(m)|^2}} \right]. \quad (3.14)$$

It should be noted that (3.14) was derived by estimating the *a priori* SNR. This leads directly to the Ephraim and Malah Noise Suppressor below.

3.2.3 The Ephraim and Malah Noise Suppressor

In [30], Ephraim and Malah presented a modification to the MLEE Filter by adding an estimator for the *a priori* SNR ($\mathcal{R}_{\text{prio}}$) which uses exponential smoothing within the time domain. An examination of the algorithm by Cappé [31] concluded that this smoothing avoids the appearance of musical noise and signal distortion. However, removal of noise is

not complete, and due to the smoothing, the signal component is incorrectly attenuated following signal transients.

Cappé summarized the Ephraim and Malah Suppression Rule (EMSR) by

$$G_{\text{EMSR}} = \frac{\sqrt{\pi}}{2} \sqrt{\left(\frac{1}{1 + \mathcal{R}_{\text{post}}}\right) \left(\frac{\mathcal{R}_{\text{prio}}}{1 + \mathcal{R}_{\text{prio}}}\right)} M \left[(1 + \mathcal{R}_{\text{post}}) \left(\frac{\mathcal{R}_{\text{prio}}}{1 + \mathcal{R}_{\text{prio}}}\right) \right], \quad (3.15)$$

where M stands for the function

$$M[\theta] = \exp\left(-\frac{\theta}{2}\right) \left[(1 + \theta) I_0\left(\frac{\theta}{2}\right) + \theta I_1\left(\frac{\theta}{2}\right) \right]. \quad (3.16)$$

In the above equation, I_0 and I_1 represent the modified Bessel functions of zero and first order. Time and frequency indices have been omitted for clarity. The *a priori* SNR is calculated by

$$\mathcal{R}_{\text{prio}}(p) = (1 - \alpha) \mathcal{R}_{\text{post}}(p) + \alpha \frac{|G(p-1)X(p-1)|^2}{|\hat{W}|^2}, \quad (3.17)$$

while the *a posteriori* SNR is the same as $\mathcal{R}(m, p)$ given by (3.12). The value of α determines the time smoothing of the *a priori* SNR estimate, which on the basis of simulations was set to about 0.98.

The *a priori* SNR is the dominant parameter, while the *a posteriori* SNR acts as a correction parameter when the *a priori* SNR is low.

In [32], Scalart and Filho examined the use of *a priori* SNR estimation with standard (Boll, Wiener and MLEE) methods and also reported reduction in the amount of musical noise. This suggests that the smoothing operation plays a more significant role in the reduction of musical noise than the gain rule.

3.2.4 Filter Smoothing

A simpler method which achieves results comparable with the Ephraim and Malah Suppression Rule is filter smoothing. The EMSR uses exponential averaging to smooth the *a priori* SNR, the dominant parameter. Since it is assumed that the noise estimate changes slowly over time, the resulting filter will also change slowly over time. A similar effect may therefore be achieved by adding exponential averaging to the filter. Using $G(m, p)$ from

Eq. (3.7), this gives

$$G_S(m, p) = \lambda_F G_S(m, p - 1) + (1 - \lambda_F) G(m, p). \quad (3.18)$$

In this equation, λ_F is used to achieve a tradeoff between the amount of musical noise and attenuation of signal transitions. As λ_F approaches 1, the amount of musical noise disappears, but signal at the onset of speech segments is lost. To overcome this effect, McAulay and Malpass described a modified form of the above in [21], where λ_F is chosen to be 0 or 0.5 depending on a comparison of the current SNR estimate to the filter gain. Similarly, the above equation can be modified to

$$G_S(m, p) = \max(\lambda_F G_S(m, p - 1) + (1 - \lambda_F) G(m, p), G(m, p)), \quad (3.19)$$

resulting in a one-sided smoothing that responds immediately to speech onset, but has a hangover dependent on λ_F . The resulting signal will sound as if originating from a reverberant space. This effect is caused by the slower decay of the filter gain after the end of the speech segment, and can be perceptually annoying. Other approaches include adapting the averaging parameter based on the spectral discrepancy measure, as proposed by Gustafsson *et al* [33].

The advantage the Filter Smoothing technique has over the EMSR is that Filter Smoothing is easier to understand and implement. Also it can be modified to take advantage of temporal auditory masking effects, as discussed in the following chapter.

3.2.5 Signal Subspace methods

A new approach to noise reduction has been discussed by Ephraim and Van Trees [34], whereby the noisy signal is decomposed into a signal-plus-noise subspace and a noise subspace. The noise subspace is removed and the signal is generated from the remaining subspace by means of a linear estimation. Ephraim and Van Trees suggested the Discrete Cosine Transform (DCT) and Discrete Wavelet Transforms as approximations to the optimal, but computationally intensive Karhunen-Loève Transform (KLT).

Subjective tests showed that some distortion was introduced to the signal, which listeners found disturbing. Partially for this reason, the attention Signal Subspace approaches have received in literature was mainly in automatic speech recognition problems.

3.2.6 Implementation of EVRC noise reduction

The Enhanced Variable Rate Coder (EVRC) is the standard coder for use with the IS-95x Rate 1 air interface (CDMA) [28, 35]. It employs an adaptive noise suppression filter, which is used as a baseline reference for the algorithm presented in this paper. Since it is a widely used “real-world” implementation of a noise reduction algorithm, it is worth examining in some detail. Some simplification for brevity was done to illustrate the algorithm more clearly, but as much as possible, the symbols used in the standard document are used.

Conceptually, the EVRC’s noise suppression is accomplished by summing the outputs of a bank of adaptive filters that span the frequency band of the input signal. The widths of the bands roughly approximate the ear’s critical bands.

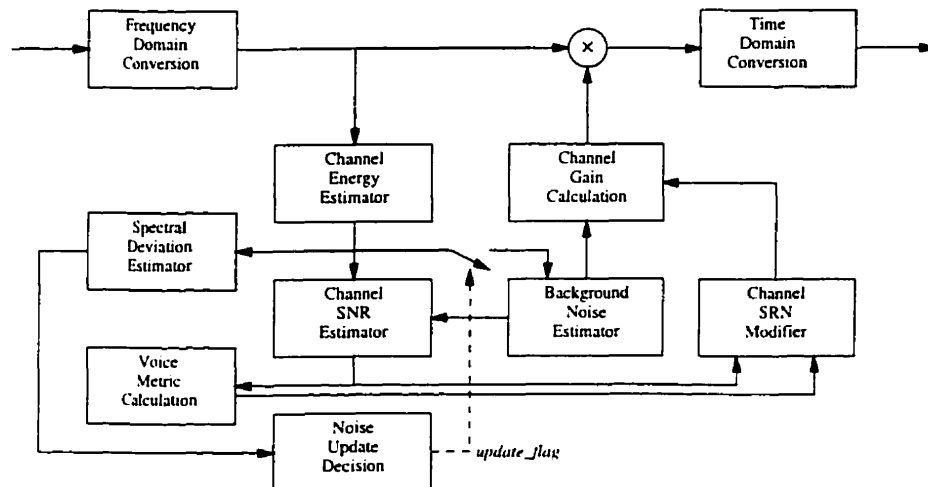


Fig. 3.6 EVRC Noise suppression structure, redrawn from [28]

The EVRC noise suppressor works on 10 ms sections of speech data, using the overlap-add method [26], to obtain 104 sample vectors. These vectors are then zero-padded to 128 sample points and transformed using a 128-point Fast Fourier Transform (FFT), windowed by a smoothed trapezoidal window. The result of the transform is denoted here as E_c . Reconstruction is done using the overlap-add method, with no windowing.

The 128 bins are grouped into 16 channels, approximating non-overlapping critical bands. The energy present in each channel is estimated by calculating the mean magnitude

for all frequency bins within the channel, and using an exponential average of the form

$$E_c(m, ch) = \frac{1}{f_H - f_L + 1} \sum_{k=f_L}^{f_H} G_m(k) \quad (3.20)$$

$$E(m, ch) = 0.45E(m-1, ch) + 0.55E_c(m, ch) \quad (3.21)$$

where m is the index of the time frame, and f_L and f_H are the lowest and highest bin respectively of that particular channel. $G_m(k)$ is the k th bin of the FFT of time frame m . Additionally, the channel energy estimate $E(m, ch)$ is constrained to a minimum of 0.0625 to prevent conditions where a division by zero occurs.

The channel energy estimate is then combined with the channel noise energy estimate (see below) to calculate the channel SNR estimate in dB units. The channel SNR values are also used to calculate a voice metric for each frame, which is used to determine if the current frame is noise only. If the frame is considered noise only, the current channel energy estimates are used to update the channel noise estimate E_N , again using exponential averaging. The channel noise estimate is constrained to a minimum of 0.0625.

$$E_N(m+1, ch) = 0.9E_N(m, ch) + 0.1E(m, ch) \quad (3.22)$$

For the final channel gain calculation, an overall gain is calculated based on the total noise energy estimate.

$$\gamma_N = -10 \log_{10} \left(\sum_{ch=0}^{15} E_N(m, ch) \right) \quad (3.23)$$

which is constrained to the range $\gamma_N = -13 \dots 0$. A quantized channel SNR is generated by

$$\sigma_Q''(ch) = \text{round} \left(10 \log_{10} \left(\frac{E(m, ch)}{E_N(m, ch)} \right) / 0.375 \right) \quad (3.24)$$

the result of which is constrained to be between 6 and 89. Now the individual channel

gains $\gamma(ch)$ can be computed.

$$\gamma_{\text{dB}}(ch) = 0.39(\sigma_Q''(ch) - 6) + \gamma_N \quad (3.25)$$

$$\gamma(ch) = \min(1, 10^{\gamma_{\text{dB}}(ch)/20}) \quad (3.26)$$

These channel gains are then applied to the FFT bins belonging to their respective channels, before the inverse FFT is performed.

However, while the EVRC noise suppressor has a concept of critical bands, it does not make use of any other perceptual properties. There is no calculation of masking thresholds, all channels are calculated independently from each other.

It should also be noted that the EVRC noise suppressor (and hence the entire coder) is preceded by a highpass filter whose 3 dB cutoff is at about 120 Hz and has a slope of about 80 dB/oct. This removes a large amount of noise which is commonly encountered in mobile applications (like car noise) while not greatly affecting speech quality.

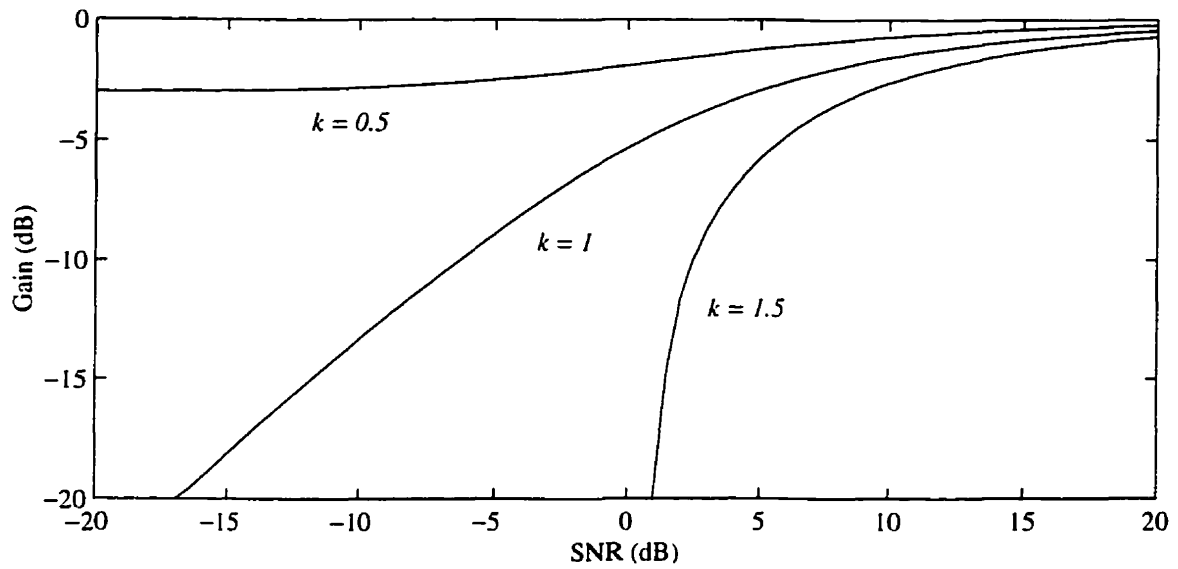
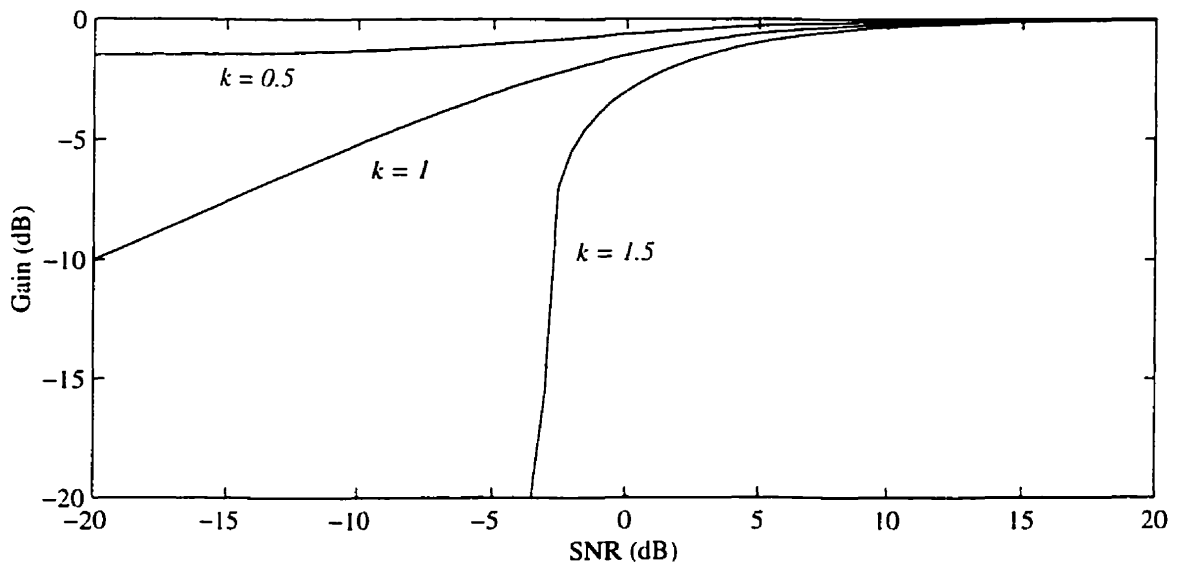
3.3 Comparison of Methods

To compare short-time spectral amplitude (STSA) subtractive methods, the *gain curve* is the primary point of comparison. The gain curve shows the attenuation of any frequency bin for any given *a posteriori* SNR, that is the value of $G(m)$ given $\mathcal{R}(m)$ from Eq. (3.12).

Figures 3.7(a) and 3.7(b) show the gain curves for magnitude and power spectral subtraction respectively. From the plots, it can be seen that the parameter k is dominant in determining the slope of the curve. For small k the attenuation remains small even for very low SNR values. For $k = 1.5$ (in general, for $k > 1$), the spectral subtraction algorithm (for either value of a) acts more as a noise gate, cutting off completely (assuming $\alpha = 0$) if the SNR drops below

$$\mathcal{R}_{\text{off}} = 10 \log_{10}(k^{\frac{a}{2}} - 1) \quad (\text{dB}), \quad k > 1. \quad (3.27)$$

Figure 3.8 shows the gain curves of some of the other methods described in the previous section. As expected the curve for the Wiener filter is very similar to the power spectral subtraction with $k = 1$. It is an interesting feature of the Wiener filter that as the SNR decreases, the filter gain becomes equal to the SNR.

(a) Magnitude Spectral Subtraction ($a = 1$)(b) Power Spectral Subtraction ($a = 2$)**Fig. 3.7** Gain curves of spectral subtraction algorithms

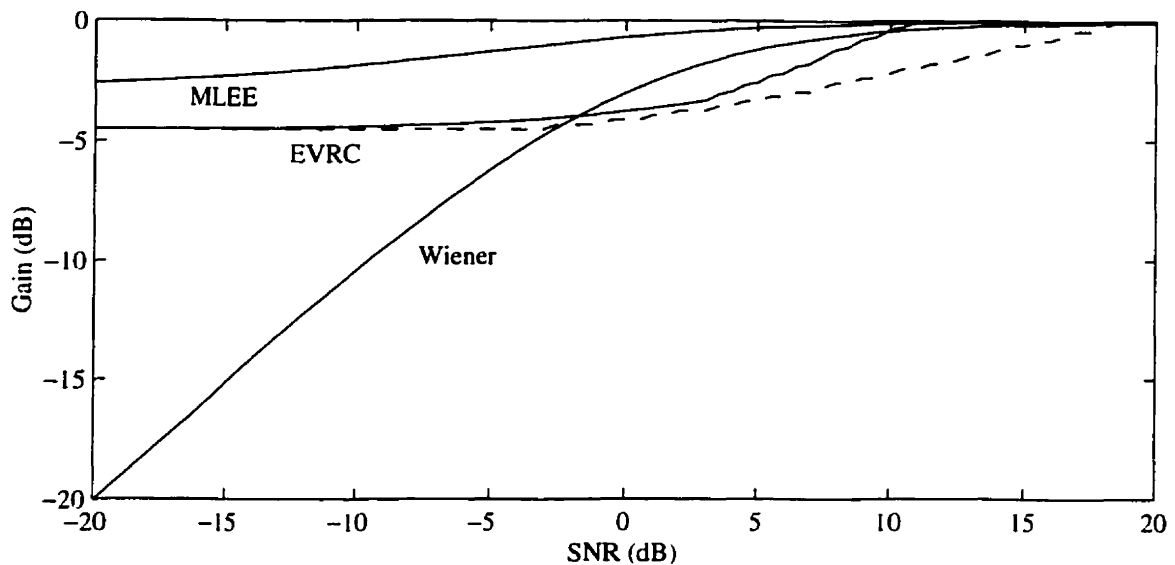


Fig. 3.8 Gain curves of selected other methods

The other curves on Fig. 3.8 show the gain curves for the MLEE method and the EVRC noise suppressor. The MLEE curve provides very little attenuation, with a maximum attenuation of 3 dB. It is therefore of little use if the intent is to provide significant noise removal.

For reference, the EVRC noise suppressor was included. Like the Ephraim and Malah Noise Suppressor, the gain is dependent not only on the (*a posteriori*) SNR, but on other values as well. In the case of the EVRC noise suppressor, the gain is not only subject to temporal smoothing, but also on the overall estimate of the noise, as can be seen from equations (3.23)–(3.26). The two EVRC curves on fig. 3.8 show the gain assuming fixed signal power, but varying noise power (solid line) and fixed noise but varying signal power (dotted line). Both curves are based on the noise power being constant across the whole spectrum.

3.4 Summary

In this chapter, some methods for reducing or removing acoustic noise are introduced. In particular, methods based on short-time fourier transforms are examined. The problems of window effects and noise estimation are briefly discussed. The artifacts introduced by STSA

methods are described, and how the spectral subtraction method is modified to counter these artifacts. The EVRC noise suppression algorithm is discussed in some detail. This gives insight into a “real-world” implementation of a noise reduction algorithm. Finally, some of the methods were compared based on the attenuation given an estimate of the SNR.

Chapter 4

Using Masking Properties in Spectral Subtraction Algorithms

Auditory masking is aggressively exploited by algorithms used for the lossy compression of audio signals. In compression of audio signals, the intent is to hide the noise introduced by the coding below the masking threshold, thus making the noise inaudible. This will then render the coding process transparent, enabling better compression without audible degradation of the signal. A comprehensive review of perceptual audio coding was published by Painter and Spanias [5].

More recently, masking properties of the ear have also been used to improve the quality of noise reduction algorithms. Specifically, instead of attempting to remove all noise from the signal, these algorithms attempt to attenuate the noise below the audible threshold. In the context of short-time spectral magnitude (STSM) subtractive algorithms, this reduces the amount of modification to the spectral magnitude, reducing artifacts. This is of great importance where the resulting signal needs to be of very high quality. The methods developed by Soulodre [4] to remove camera noise from film soundtracks were used as a starting point for the method presented in this chapter. In fact, it may be regarded as an application of Soulodre's methods to more general noise reduction.

For the design of audio coders, an estimate of the masking threshold must be calculated. In this chapter, some of the masking models (or *perceptual models*) will be examined. Also, it will be shown how these models are used in noise suppression algorithms.

4.1 Masking Models

4.1.1 The Johnston Model

A perceptual model was developed by Johnston for coding of audio sampled at 32 kHz in [36]. This model was used by Tsoukalas *et al* in [6] for speech enhancement and is described below. Johnston's method calculates the auditory masking threshold to determine how much noise the coder can add before it becomes audible.

Johnston uses the following steps to calculate the masking threshold;

- Critical band analysis of the signal
- Applying the spreading function to the critical band spectrum
- Calculating the spread masking threshold
- Relating the spread masking threshold to the critical band masking threshold.
- Accounting for absolute thresholds

Johnston's coder operates on 32 kHz sampled signals, and transforms 2048 samples (64 ms) in each frame. This results in an internal frequency resolution of 15.625 Hz. A Hanning window is used to overlap the frames, which are 1920 samples long (6.25% overlap between frames).

Critical Band Analysis

The first step calculates the energy present in each critical band, assuming discrete nonoverlapping critical bands. This is similar to the method used by the EVRC Noise Suppressor as discussed in Section 3.2.6. The summation

$$B(i) = \sum_{m=b_l(i)}^{b_h(i)} |X(m)|^2, \quad i = 1, \dots, i_{\max}. \quad (4.1)$$

where $b_l(i)$ and $b_h(i)$ are the lower and upper boundaries of the i^{th} critical band, differs from Eq. (3.21) only by not including a normalization for the number of DFT bins summed. The value of i_{\max} depends on the sampling frequency.

Johnston notes that a true critical band analysis would calculate the power within one critical band at every frequency m . This would create a higher resolution critical band spectrum. In the context of the coder, (4.1) represents an adequate approximation.

Spreading Function

To calculate the excitation pattern, Johnston uses the spreading function as proposed by Schroeder *et al* in [37]. The spreading function $S(i)$ has lower and upper skirts of +25 dB/Bark and -10 dB/Bark respectively. It is a reasonable approximation (at intermediate speech levels) to the experimental data given by Zwicker [10], as shown in Fig. 2.4. This spreading function is then convolved with the bark spectrum, to give

$$C(i) = S(i) * B(i), \quad (4.2)$$

where $C(i)$ denotes the spread critical band spectrum.

Calculation of the Noise Masking Threshold

Two masking thresholds are used, one for a tone masking noise and another for noise masking a tone. Tone-masking-noise is estimated at $14.5+i$ dB below $C(i)$. Noise-masking-tone is estimated as being a uniform 5.5 dB below $C(i)$ across the whole critical band spectrum.

To determine if the signal is tonelike or noiselike, the Spectral Flatness measure (SFM) is used. The SFM (in decibels) is defined as

$$SFM_{dB} = 10 \log_{10} \frac{G_m}{A_m}. \quad (4.3)$$

where G_m and A_m represent the geometric and arithmetic mean of the power spectrum respectively. From this value, a totality coefficient α is generated, by

$$\alpha = \min \left(\frac{SFM_{dB}}{SFM_{dBmax}}, 1 \right), \quad (4.4)$$

where $SFM_{dBmax} = 60$ dB represents the SFM of an entirely tonelike signal, resulting in a tonality coefficient of $\alpha = 1$. Conversely, an entirely noiselike signal would have $SFM_{dB} = 0$ and thus $\alpha = 0$.

Using α , the offset in decibels for each band is calculated as

$$O(i) = \alpha(14.5 + i) + (1 - \alpha)5.5. \quad (4.5)$$

This offset is then subtracted from the spread critical band spectrum in the dB domain by

$$T(i) = 10^{\log_{10}(C(i)) - (O(i)/10)}. \quad (4.6)$$

To reduce complexity, Virag [8] uses a simplified method proposed by Sinha and Tewfik in [38]. The simplified model is based on the idea that the speech signal has a tonelike nature in lower critical bands and a noiselike nature in higher bands.

Converting the Spread Threshold back to the Bark Domain

This step attempts to undo the convolution of $B(i)$ with the spreading function. Due to the shape of the spreading function this process is very unstable, and thus a renormalization is used instead. The spreading function increases the energy estimates in each band. The renormalization multiplies each $T(i)$ by the inverse of the energy gain, assuming a uniform energy of 1 in each band. The renormalized $T(i)$ is denoted $T'(i)$.

Including the Absolute Threshold

The final step is to compare $T'(i)$ to the absolute threshold of hearing. Since the actual playback level is not known, it is assumed that the playback level is set such that the quantization noise is inaudible. Specifically, it is assumed that a signal of 4 kHz with peak magnitude of ± 1 least significant bit of a 16 bit integer value is at the absolute threshold of hearing (-5 dB SPL at 4 kHz). Thus, the final threshold is computed as

$$T_J(m) = \max\left(T'(z(f_s \frac{m}{M})), T_q(f_s \frac{m}{M})\right), \quad (4.7)$$

where $z(f)$ is a function to convert from linear frequency to Bark, as defined by Eq. (2.2). $T_q(f)$ is the threshold of hearing as defined by Eq. (2.1), and $f_s \frac{m}{M}$ is the center frequency of the m^{th} frequency bin.

4.1.2 The Perceptual Audio Quality Measure

A more detailed model of the auditory system was developed by Beerends and Stemerding in [39] to measure the quality of audio devices. Interestingly this model was also applied by Tsoukalas *et al* in [7] for *audio* signal enhancement. The following describes the implementation by Tsoukalas *et al*.

The primary differences between the Perceptual Audio Quality Measure (PAQM) and Johnston's method (described above) are the inclusion of temporal masking estimates, more detailed spreading functions, and a calculation of compressed loudness. There is no calculation of tonality of the signal. The difference in masking between tonelike and noiselike sounds is instead accounted for by the compressed loudness function.

The implementation by Tsoukalas *et al* is actually a greatly simplified version of PAQM and can be summarized in two steps. The first step is the conversion to Bark domain, as in the Johnston model by Eq. (4.1). Restating (4.1) with time indices added, we get

$$B(i, p) = \sum_{m=b_l(i)}^{b_h(i)} |X(m, p)|^2, \quad i = 1, \dots, i_{\max}. \quad (4.8)$$

The second step is to calculate the (noncompressed) excitation pattern by

$$X_f(i, p) = \sum_{\nu=0}^{i_{\max}} \left\{ SS(\nu, i) a_0(\nu) \sum_{k=0}^p [T_f^{p-k}(\nu) B(\nu, k)] \right\}, \quad i = 1, \dots, i_{\max}. \quad (4.9)$$

In the above equation, $a_0(i)$ represents an outer-to-inner ear transformation, and $T_f(i)$ is an exponential function given by

$$T_f(i) = e^{-d/\tau(i)}. \quad (4.10)$$

which accounts for time-domain spreading. In (4.10), d is the time distance between adjacent short-time frames and $\tau(i)$ is derived from time-domain masking experiments. The function $SS(\nu, i)$ is defined as

$$SS(\nu, i) = \begin{cases} S_2(\nu, i - \nu) & \nu < i, \\ S_1(\nu - i) & \nu \geq i, \end{cases} \quad (4.11)$$

where S_1 is the lower spreading function and S_2 the upper spreading function. Beerends and Stemerdink used

$$S_1 = 31 \text{ dB/Bark}, \quad (4.12)$$

$$S_2 = 22 + \min(230/f, 10) - 0.2L \text{ dB/Bark}, \quad (4.13)$$

with f the frequency of the masker in hertz and L the level in dB SPL. Tsoukalas *et al* dropped the level dependence.

4.1.3 Soulodre's Model

For the purpose of removing camera noise from soundtracks, Soulodre [4] developed a model which operates in the linear frequency domain, thus retaining the high frequency resolution of the DFT.

The modeling of the outer and middle ear is performed by

$$A_S = -6.5e^{-0.6(f-3.3)^2} + 0.001f^4 + 3.64f^{-0.8} - 80.64e^{-4.712f^{0.5}} \text{ (dB)}, \quad (4.14)$$

where f is in kHz, and the internal noise of the auditory system is modeled by

$$N_{\text{int}} = 80.64e^{-4.712f^{0.5}} \text{ (dB)}. \quad (4.15)$$

It should be noted that by adding these two equations, the absolute threshold of hearing as stated in (2.1) is modeled.

The auditory filter model is based on the research of Patterson and Moore, but the complete model is original to Soulodre [4]. This model uses the Roex(p) (rounded exponential) filter shapes for the auditory filter approximations. The response is described by

$$W(g) = (1 + pg)e^{-pg}, \quad (4.16)$$

where g is the normalized distance from the center frequency f_0 of the filter evaluation point.

$$g = \frac{|f - f_0|}{f_0}. \quad (4.17)$$

The parameter p determines the slopes of the filter and thus its bandwidth. To find the value of p , the Roex(p) filters are expressed in terms of their effective rectangular bandwidth (ERB). The ERB's for auditory filters are given by the expression [13]

$$\text{ERB} = 24.7(4.37f + 1), \quad (4.18)$$

where f is in kHz. By equating the area under the curves of the Roex(p) and rectangular filters, it is possible to derive p as

$$p = \frac{4f_0}{24.7(4.37f_0 + 1)}. \quad (4.19)$$

Thus, the excitation pattern across frequency due to a signal at frequency f_c is obtained by

$$\mathcal{J}(f_c, f) = \left(1 + \frac{4|f_c - f|}{24.7(4.37f + 1)}\right) e^{-\frac{4|f_c - f|}{24.7(4.37f + 1)}}. \quad (4.20)$$

To account for variations in the shape of the auditory filter with level, the parameter p for the low-frequency skirt of the filter is adjusted by

$$p_{l(X)} = p_{l(51)} - 0.38 \left(\frac{p_{l(51)}}{p_{l(51.1k)}} \right) (X - 51). \quad (4.21)$$

where $p_{l(51)}$ is the value of p at the center frequency for an equivalent noise level of 51 dB/ERB and $p_{l(51.1k)}$ is the value of p_l at 1 kHz for a noise level of 51 dB/ERB. The parameter X denotes the equivalent input noise level in dB/ERB.

To predict nonsimultaneous masking, the model

$$\text{FM}(L_m) = a(b - \log \Delta t)(L_m - c) \text{ dB SL} \quad (4.22)$$

is used, where a , b , and c are made to fit experimental data, Δt is the length of the delay between the masker and the signal, and L_m is the level of the masker in terms of sensation level (SL). As with other model described in this chapter, backward masking is ignored.

To simplify the calculating process, Δt was fixed and the experimental data was fit to

$$\text{FM}(f, L) = \alpha(L) + \beta(L)e^{-\frac{f}{\gamma(L)}}, \quad \begin{array}{l} 100 \text{ Hz} \leq f \leq 20 \text{ kHz}, \\ 10 \text{ dB SPL} \leq L \leq 100 \text{ dB SPL}. \end{array} \quad (4.23)$$

For frequencies below 100 Hz, the value predicted at 100 Hz should be used, and for masker levels below 10 dB SPL, a value of 0 should be assigned to $\text{FM}(f, L)$.

The masking components, both simultaneous and non-simultaneous, are added using a modified power-law. It can be expressed as

$$M = 10 \log \left[\left(\left[\sum_{i=1}^N (10^{M_i/10})^\rho \right] - (10^{T_q/10})^\rho \right)^{1/\rho} \right], \quad (4.24)$$

where $M_i = 1, 2, \dots, N$ are the levels of the various masking components, T_q is the absolute threshold of hearing, and ρ is the compression factor. Setting $\rho = 0.3$ was found to give a good fit to the experimental data when predicting masking thresholds.

4.1.4 Perceptual Evaluation of Audio Quality

A new psychoacoustic model was developed by the International Telecommunications Union (ITU) for use in a standard for objective measurement of perceived audio quality (adopted as ITU-R BS.1387) [16, 40]. An evaluation of this method performed by Treurniet and Soulodre [41] found that this measure produced results that correlate well with subjective ratings obtained in formal listening tests. As with the PAQM above, the full model is not described here. The following description covers only the parts that are necessary in the context of noise reduction algorithms. However, since this masking model is implemented for use by the noise reduction methods described in the following sections, the calculation of the excitation pattern and the masking threshold will be covered in detail.

The Perceptual Evaluation of Audio Quality (PEAQ) model consists of two versions: one that is intended for applications requiring high processing speed, called the basic version, and another for applications requiring highest achievable accuracy, called the advanced version. The basic version only uses an FFT-based ear model, whereas the advanced version uses an FFT-based model to determine the masking threshold and a filter bank based ear model to compare internal representation. Only the basic version (specifically, the estimation of the masking threshold thereof) is used in the proposed noise suppression

algorithm. The basic version of PEAQ is very similar to PAQM.

The steps involved in computing the excitation pattern in the basic version are as follows.

- Time to Frequency conversion
- Frequency-dependent weighing
- Mapping into perceptual (Bark) domain
- Adding internal noise
- Applying the spreading function
- Applying nonlinear superposition
- Temporal Spreading

Time to Frequency Conversion

PEAQ was designed for the comparison of audio devices over the the whole audible spectrum, and therefore operates on signals sampled at 48 kHz. The transform size is 2048 samples with 50% overlap, thus working on 0.021 s time increments. This results in a frequency resolution of $\Delta_f = 23.4375$ Hz. Following the transform, the level is scaled to a level assuming the maximum level to be 92 dB SPL.

Frequency-dependent weighting function

The outer and middle ear are modeled by the frequency dependent weighting function

$$A(f) = -0.6 \cdot 3.64f^{-0.8} + 6.5e^{(f-3.3)^2} - 10^{-3}f^{3.6} \text{ (dB)}, \quad (4.25)$$

where f is in kHz. Using $X(m)$ as the transformed input signal, the weighted spectrum is

$$X_w(m) = |X(m)| \cdot 10^{\frac{A(f(m))}{20}}. \quad (4.26)$$

where $f(m) = (m\Delta_f)/1000$ is the center frequency (in kHz) of the m^{th} frequency bin.

Mapping into perceptual domain

The weighted power spectrum, $|X_w(m, p)|^2$, is transformed into the perceptual domain. Specifically, the energy is grouped into 0.25 Bark bands. It should be noted that PEAQ uses a slightly different frequency warping function than Eq. (2.2), and instead uses [37]

$$z = 7 \cdot \operatorname{arcsinh} \left(\frac{f}{0.65} \right) \text{ (Bark)}, \quad (4.27)$$

where f is in kHz. The resulting frequency bands are listed in Appendix A.

Adding internal noise

With the signal in perceptual domain (denoted $P_E(k)$), the internal auditory noise $N_I(k)$ is added. The noise is modeled by

$$P(k) = P_E(k) + N_I(k) = P_E(k) + 10^{0.4 \cdot 0.364 \cdot (f_c(k))^{-0.8}}, \quad (4.28)$$

where $f_c(k)$ represents the center frequency (in kHz) of the k^{th} perceptual band. This noise floor will also account for the absolute threshold of hearing.

Spreading function

A spreading function is applied to the perceptual spectrum, similar to PAQM. The slopes are slightly different, with

$$S_1(k, L(k)) = 27 \text{ dB/Bark}, \text{ and} \quad (4.29)$$

$$S_2(k, L(k)) = 24 + \frac{0.23}{f(k)} - 0.2L(k) \text{ dB/Bark}. \quad (4.30)$$

where $L(k)$ represents the signal power (in dB SPL) in the k^{th} perceptual band.

Nonlinear superposition

The spread perceptual bands are added in a nonlinear normalized summation (described in [40], section 2.1.7, here denoted by the operation norm_k)

$$E_2(k) = \text{norm}_k \left(\sum_i (E_S(i, k))^\alpha \right)^{1/\alpha}, \quad (4.31)$$

where $E_S(i, k)$ represents the energy spread of the i^{th} band to the k^{th} band. The parameter α was chosen to be 0.4 following an experimental optimization process [16]. E_2 is called the *unsmearred excitation pattern*.

Temporal spreading

The final step in calculating the excitation pattern is taking account of temporal spreading. As mentioned in Sec. 2.2.2, only forward masking is taken into account. The time constants depend on the center frequency of each band and are calculated by

$$\tau(k) = \tau_{\min} + \frac{0.1}{f(k)} (\tau_{100} - \tau_{\min}), \quad (4.32)$$

where $\tau_{100} = 0.030$ s and $\tau_{\min} = 0.008$ s. As above, $f(k)$ is in kHz. The spreading is applied to the unsmearred excitation pattern E_2 by the exponential averaging

$$E_f(k, p) = a(k)E_f(k, p-1) + (1 - a(k))E_2(k, p) \quad \text{and} \quad (4.33)$$

$$E(k, p) = \max(E_f(k, p), E_2(k, p)), \quad (4.34)$$

where p is the frame (time) index, and

$$a(k) = e^{-\frac{3}{187.5\tau(k)}}. \quad (4.35)$$

$E(k, p)$ is the *excitation pattern*, which is sufficient for some methods. A masking threshold can be computed from the excitation pattern by applying the weighing function

$$m(k) = \begin{cases} 3.0 & k \leq 12 \\ 0.125k & k > 12, \end{cases} \quad (4.36)$$

(noting that $k = 0.25$ Bark) yielding

$$M(k, p) = \frac{E(k, p)}{10^{m(k)/10}}, \quad (4.37)$$

which is the *mask pattern*.

4.2 Perceptual based noise reduction

The use of perceptual models in acoustic noise suppression was already proposed by Petersen and Boll in [42]. Although a simplistic model (by modern standards) for estimating the masking threshold was used, Petersen and Boll reported that their method greatly reduced the artifacts introduced by spectral subtraction. However, the method described in [42] is not a STSM based method. In [43], Cheng and O'Shaughnessy also propose two algorithms that exploit auditory properties, but are not STSM based.

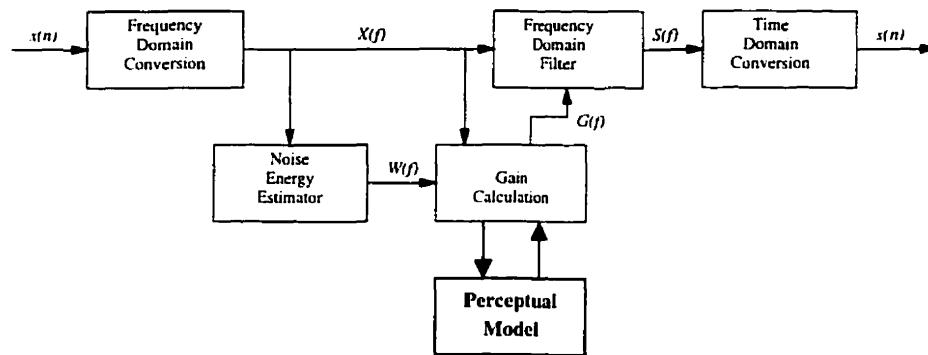


Fig. 4.1 Incorporating a perceptual model in a spectral subtraction algorithm

The focus of this section is on methods combining STSM subtractive methods with auditory models as described above. The auditory model usually affects the Gain Calculation only (see Fig. 4.1). A new method is presented in the following section, by combining the PEAQ masking model with a modified form of the zero-phase spectral subtraction filter proposed in [4]. Other methods (described below) are also implemented using the PEAQ auditory model, and are compared to the proposed method.

4.2.1 Tsoukalas' method for Speech Enhancement

Soulodre derives his method from the work of Tsoukalas *et al.* The method described in [6, 44] for speech enhancement is summarized by Soulodre [4] as

$$|\hat{S}(f)|^2 = |X(f)|^2 - \max(|\hat{W}(f)|^2 - \text{AMT}, 0), \quad (4.38)$$

where AMT is the Auditory Masking Threshold given by an estimate of the clean signal. It should be noted that rather than direct spectral modification, Tsoukalas *et al* calculate the parameters of the nonlinear gain function

$$G_{\text{T}}(m, p) = \frac{|X(m, p)|^{2v(m, p)}}{a^{v(m, p)}(m, p) + |X(m, p)|^{2v(m, p)}}, \quad (4.39)$$

where $a(m, p)$ and $v(m, p)$ are the time-frequency varying parameters. This nonlinear gain function is based on a function proposed by Eger *et al* in [45], and was further developed by Clarkson and Bahgat [46]. In the above method, $a(m, p)$ is a threshold below which all frequency components are highly suppressed, and $v(m, p)$ controls the rate of suppression. Tsoukalas *et al* found the influence of $v(m, p)$ negligible and fixed it at $v(m, p) = v = 1$. The parameter $a(m, p)$ is constrained to be constant within a critical band. and Tsoukalas *et al* present various ways of calculating $a_{\text{CB}}(i, p)$, such as

$$a_{\text{CB}}(i, p) = (\hat{W}_{\text{CB}}(i) + T_{\text{J}}(i)) \left(\frac{\hat{W}_{\text{CB}}(i)}{T_{\text{J}}(i)} \right)^{1/v}. \quad (4.40)$$

where $\hat{W}_{\text{CB}}(i)$ represents the noise in the i^{th} critical band and $T_{\text{J}}(i)$ represents the AMT (using Johnston's method) in the i^{th} critical band. To obtain a good estimate of the AMT Tsoukalas *et al* suggest an iterative approach, at the expense of computational efficiency. Essentially, the first AMT is obtained using standard power spectral subtraction, and \hat{S} is obtained using (4.39). The AMT is calculated using \hat{S} , and (4.39) is applied to \hat{S} . The parameter $a_{\text{CB}}(i, p)$ will decrease with each iteration, converging towards zero, thus indicating no more suppression is needed.

Tsoukalas *et al* report that to begin the iterative process, even the noisy signal can be used to find the AMT. However, more iterations must be performed for $a_{\text{CB}}(i, p)$ to converge.

4.2.2 Musical Noise Suppression

A more direct method for suppressing the musical noise that is generated by STSM subtractive methods was presented by Haulick *et al* in [9]. Conceptually, this algorithm acts as a postprocessor to conventional spectral subtraction. The masking thresholds for the noisy signal and the output signal are computed. Components that are audible (above the masking threshold) in the output but not the input are candidates for suppression. To avoid suppressing previously inaudible unvoiced speech segments, a short-time stationarity and bandwidth criterion is applied. In order to be classified as musical, noise must have a bandwidth of less than about 300 Hz. If two successive filter coefficients fulfill the condition

$$\min (G_H(m, p - 1), G_H(m, p)) \geq 0.55, \quad (4.41)$$

the corresponding spectral component is assumed be speech and is not suppressed. Audible spectral components that meet the criteria for musical noise are suppressed by setting the corresponding filter coefficient to the noise floor β .

4.2.3 Virag's method

A method developed by Virag [8] can be viewed as a lower complexity version of the speech enhancement method by Tsoukalas *et al*, though it is not directly derived from it. Virag uses the masking threshold estimate (obtained using power spectrum subtraction) to adjust the spectral subtraction parameters k and α of Eq. (3.7) on a per-band and per-frame basis. The adaption of the subtraction parameters is performed with

$$k(m) = F_k[k_{\min}, k_{\max}, T(m)] \quad (4.42)$$

$$\alpha(m) = F_\alpha[\alpha_{\min}, \alpha_{\max}, T(m)], \quad (4.43)$$

where k_{\min} , k_{\max} , α_{\min} , and α_{\max} constrain k and α , and $T(m)$ is the masking threshold estimate. The functions F_k and F_α lead to maximal residual noise reduction for minimal masking threshold and vice versa, such that $F_k = k_{\max}$ if $T(m) = T(m)_{\min}$ and $F_k = k_{\min}$ if $T(m) = T(m)_{\max}$. $T(m)_{\min}$ and $T(m)_{\max}$ are the minimal and maximal values of the masking threshold respectively, updated from frame to frame. To avoid discontinuities in the gain function, a smoothing function is applied.

Virag found that $k_{\min} = 1$, $k_{\max} = 6$, $\alpha_{\min} = 0$, and $\alpha_{\max} = 0.02$ gives a good tradeoff between residual noise and speech distortion.

Earlier, a similar approach was taken by Lorber and Hoeldrich in [47], for use in audio restoration. However, a very simplified auditory model (consisting of only an approximation of the spreading function) was used, to smooth an estimate of the SNR. The SNR estimate was then used to calculate α in a similar fashion to Virag's method.

4.2.4 Tsoukalas' method for Audio Signal Enhancement

Simultaneously to the method described in Sec. 4.2.1, Tsoukalas *et al* derived a method for the more general problem of noise removal from audio signals. An example of an application is the restoration of phonograph recordings. In [7], a more sophisticated auditory model is used, based on PAQM (see Sec. 4.1.2).

To obtain a signal with the same psychoacoustic representation as the clean signal, Tsoukalas *et al* state that the ideal filter is

$$G_{\text{PT}} = \frac{PE(S)}{PE(X)}, \quad (4.44)$$

where $PE(\cdot)$ represents applying a perceptual model (usually by calculating the excitation pattern) to a signal. In the absence of the psychoacoustic representation of the clean signal, the filter is instead calculated as

$$G_{\text{PT}} = 1 - \frac{PE(\hat{W})}{PE(X)}. \quad (4.45)$$

It should be noted that the noise estimate is relatively fixed for music type audio signal enhancement. Since the perceptual model in the numerator only needs to be recomputed when the noise estimate is modified, this reduces the computational complexity.

4.2.5 Soulodre's method

When evaluating the method presented in the preceding section, Soulodre points out in [4] that the method in [7] ignores the fact that the width of the auditory filters (and hence the amount of masking) varies significantly with level. Essentially, Eq. (4.45) subtracts the psychoacoustic representation of the noise, and this is inconsistent with the nonlinear

addition of masking.

Instead, Soulodre proposes a filter based on (4.44),

$$G_s = \frac{PE(|S|)}{PE(|X|)} = \frac{PE(|X| - |\hat{W}|)}{PE(|X|)}. \quad (4.46)$$

Essentially, an initial estimate of the spectral magnitude of the clean signal is made using a traditional spectral subtraction algorithm. The perceptual model described in Sec. 4.1.3 was developed for use with this method.

Effects of windows

Perhaps the most important observation of Soulodre is the effect of the window on perceptual noise reduction algorithms. As discussed in Sec. 3.1.3, the window is of little importance in traditional STSA subtractive algorithms. However, the frequency domain smearing caused by the window of the Discrete Fourier Transform (DFT) [27] can be very broad. Soulodre points out that the sine window, used by many perceptual codecs, can cause the masking threshold to be overestimated.

Soulodre instead proposes the Kaiser-Bessel Derived (KBD) windows, developed for the Dolby AC-3 audio codec and used in the MPEG AAC codec [5]. At the expense of some passband selectivity, the KBD windows provide better stopband attenuation, the tradeoff controllable by a parameter.

A further refinement in Soulodre's method is the adjustment of the auditory filter slopes in the model to account for the wider main lobe of the KBD window. Since Soulodre's model uses Roex(p) filters, the modified filters are described by (see Eq. (4.16))

$$W(g) = (1 + \tilde{p}g)e^{-\tilde{p}g}, \quad (4.47)$$

where $\tilde{p} \geq p$ is a modified version of p to account for the effects of the chosen window.

4.3 Using the PEAQ model in noise reduction

The perceptual noise reduction methods discussed above were mostly intended for use in speech enhancement. Exceptions are Soulodre's method and Tsoukalas' method for audio enhancement, to which Soulodre's method is closely related. As discussed in the

introduction, methods aimed at speech enhancement tend to place a higher emphasis on noise reduction at the expense of distortion of the signal.

In this section, the implementation of Souloudre's method coupled with the PEAQ (see Sec. 4.1.4) auditory model is presented as a novel noise reduction method that attempts to provide significant noise reduction without perceivable signal distortion. This approach is hereafter referred to as Perceptual Noise Ratio Filter (PNRF).

While the other methods presented above were originally implemented using different masking models, this makes comparison of the methods difficult. Since the focus of this thesis is more on noise reduction methods rather than the auditory models, the methods described in the above section were implemented using the same auditory model.

4.3.1 Choice of Masking Model

The PEAQ auditory model from ITU-R BS.1387 was chosen as the masking model since by virtue of being from a recognized standard, it is unambiguously defined and well tested [41]. Also, its similarity to the Johnston model (which is primarily used in speech oriented methods) and PAQM allows its integration with noise reduction methods based on these perceptual models.

While Souloudre's auditory model offers the advantage of being in the linear frequency domain, it is not completely specified in [4]. It is also computationally more complex, requiring calculation of all frequency bins, whereas perceptually based models group many bins in the higher frequencies.

4.3.2 PNRF Implementation

Figure 4.2 shows how the PNRF method is implemented, as the internals of the "Gain Calculation" block of Figure 3.1. In this figure, the "ITU Perceptual Model" represents the calculation of the excitation pattern as described in Section 4.1.4. Since the excitation pattern is calculated in the perceptual domain, the ratio of the excitation patterns must be converted back into the linear domain, as described below¹. The resulting filter is smoothed with $\lambda_F = 0.01$, and constrained to a minimum of $\alpha = 0.1$ to further reduce musical noise.

¹Note that the excitation patterns are never zero due to the internal noise, and thus the division is always defined

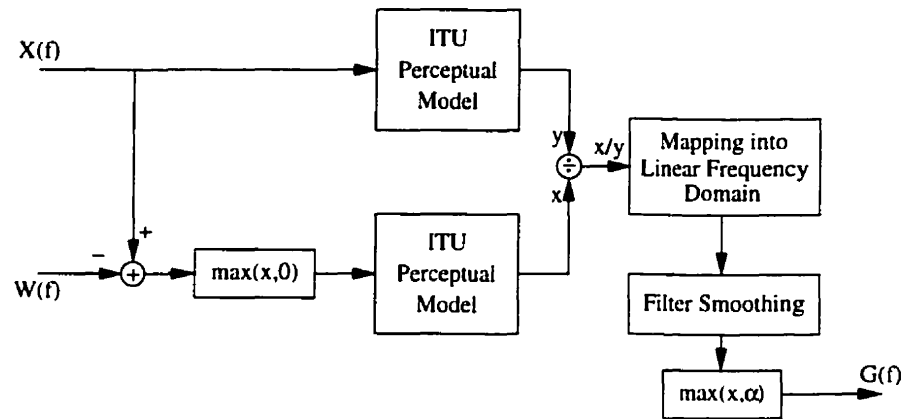


Fig. 4.2 Implementation of PNRF Gain Function

4.3.3 Implementation Issues

All methods were implemented using the same time- to frequency-domain conversion, based on the requirements for the PEAQ model. The size of the DFT is chosen such that the bin spacing (f_s/M , see Sec. 3.1.1) does not exceed the bandwidth of the smallest group in the auditory model (in the case of PEAQ, 23.445 Hz). Also, the order of the DFT should be a power of 2, such that the more efficient *Fast Fourier Transform* (FFT) can be used [26]. Overlap between frames is set at 50%, using a Hanning window, as specified by the PEAQ model.

When used at a sampling frequency of $f_s = 8000$ Hz, frames are spaced 256 samples (32 ms) apart. For audio processing, sampling frequency being either $f_s = 44100$ Hz or $f_s = 48000$ Hz, frames are spaced 1024 samples (23.22 ms and 21.33 ms respectively) apart.

Since for testing the clean signal was available, the problem of accurate speech detection (by use of a VAD, see Sec. 3.1.5) could be avoided. Instead, the clean signal was used to determine periods of speech activity, though the noise estimate was obtained from the noisy signal. For the noise estimate, a forgetting factor of $\lambda_N = 0.97$ (equivalent to a time constant of about 33 frames, or about 1 s) was used.

4.3.4 Parameters and Modifications

For methods with adjustable parameters, it was attempted to achieve a reasonable tradeoff between musical noise, residual noise, and signal distortion.

Boll's noise suppression method, required by the algorithm proposed by Haulick *et al.*, also serves as a good reference point for evaluation of auditory based methods. The parameters used are $a = 2$ for power spectral subtraction, an oversubtraction factor $k = 1.5$, and a spectral floor $\alpha = 0.1$. Of note is especially the high value of $\alpha = 0.1$, which is based on preliminary testing, where the musical noise was deemed to be more disturbing than the original noise.

The parameters for Virag's method are given in [8], and were kept as given. However, the "smoothing function" of $G(m, p)$ is not specified explicitly and was omitted in this implementation.

The noise suppression scheme of Tsoukalas *et al.* was implemented with some modifications. The most significant modification made was to fix the number of iterations to 4. One reason for using a fixed number of iterations was partially for computing efficiency, since this allowed all frames to be processed at once. Also, it was found that the value of a_{CB} does not always converge to zero, or do so extremely slowly, possibly due to the different auditory model. Additionally, throughout every iteration, the resulting filter was constrained to the minimum noise floor (as with Boll's method above, $\alpha = 0.1$) to avoid the signal distortion that is otherwise present. Finally, the exponent v was set to 1, as used by Tsoukalas *et al.*

Mapping from perceptual into linear domain

Most perceptually motivated methods require a mapping from the perceptual domain (in the PEAQ model, each group represents 0.25 Bark) back to the linear frequency domain. Since the denoised signal is created by use of an inverse DFT, the filter G must ultimately be in linear frequency domain. The PEAQ model was intended for the comparison of two signals, and thus there is no provision for inverse mapping the masking threshold back to SPL levels in linear domain.

At issue is if the masking threshold value calculated by the PEAQ model should be regarded as an absolute level constant within the critical band group, or if the value represents the total energy that the masked signal has to exceed within that group in order to be audible. Informal testing suggested that the former interpretation would yield better results, and thus was used in the implementation of the methods.

4.4 Summary

This chapter has presented various ways of modeling the human hearing system, most of which were intended for coding of speech or audio signals. It was shown how these auditory models were incorporated in noise suppression or speech enhancement algorithms. A new method, based on a noise suppressor originally developed for a specific problem is proposed as a good general noise suppression method. Finally, it is described how this method, and others for comparison, is implemented with one of the auditory models.

Chapter 5

Results

This chapter presents an evaluation of the enhancement techniques described in the previous chapters. Ideally, an evaluation of all the presented noise reduction methods and comparison with the proposed PNRF by formal subjective listening tests should be conducted. However, due to the complexity, time and resources required, formal testing is not feasible within the scope of this thesis. Instead, the informal testing as presented in this chapter is intended to show the potential of the methods in a real-world application.

5.1 Test data

The test data, used for both objective and subjective testing, was chosen to represent a typical application of a noise suppression system for speech enhancement. The signal consisted of four sentences, two spoken by a male and two by a female. The sentences were originally recorded separately under controlled conditions at a sampling frequency of 48 kHz, using linear 16-bit encoding. For the testing, the signal was downsampled to 8000 Hz, and the selected sentences were concatenated with a 1 s pause between each sentence.

The noise was taken from the SPIB (Signal Processing Information Base) at Rice University [48]. It consist of a recording of the interior of a automobile driving at 120 km/h, in rainy conditions. The original was sampled at 19.98 kHz using 16-bit linear encoding, and for this experiment was also downsampled to 8000 Hz.

Before adding the two signals, both were filtered by a 120 Hz highpass filter, as used by the EVRC noise suppressor. The test signals were created with SNRs of 0 dB and

6 dB, which represents comparatively high noise levels (in contrast, the objective measures to assess SNR improvement for the AMR noise suppressor (GSM 06.78, annex E) specify test signals using car noise in the range of 3 dB to 15 dB SNR [49]). For the purposes of calculating the level at which noise is added to the speech, the speech level was calculated according to ITU-T recommendation P.56 [50].

5.2 Objective Comparisons

Objective quality comparisons of speech are intended to predict the preference a human listener would indicate. The results of an ideal objective measure would be indistinguishable from those obtained from human observers. This means the objective comparison method would require knowledge of all levels of human speech processing, such as psychoacoustics, acoustic-phonetics, syntax, semantics, etc. Since most speech processing systems (either coders or noise reduction systems) do not produce distortions in the higher levels of perception (such as syntax or semantics), these aspects can generally be ignored when comparing signals produced from the same initial unprocessed signal [51].

While there are objective measures incorporating psychoacoustic models (the masking models described in Sections 4.1.2 and 4.1.4 are from such methods), in this chapter only *basic* objective quality measures are used. Basic objective measures, such as the Signal-to-Noise Ratio (SNR) and the Segmental SNR (SNR_{SEG}) used below, are compactly computable functions that can be uniformly applied to all forms of speech distortion in order to estimate subjective quality [51].

SNR measures are generally applicable only in sample-by-sample based processing systems, and while not good at comparing dissimilar distortions, generally perform well when ranking similar distortions. SNR measures are not able to provide fine distinctions.

In the following evaluations, three noise measures are used. SNR, SNR_{SEG}, and SNR Improvement (SNR_{IMPR}). Of these, the first two are commonly used to evaluate waveform coders, while the last is specific to evaluating noise reduction methods. The SNR is defined as

$$\text{SNR} = 10 \log_{10} \frac{\sum_n |s(n)|^2}{\sum_n |s(n) - \hat{s}(n + \Delta_p)|^2} \quad (\text{dB}). \quad (5.1)$$

where $s(n)$ and $\hat{s}(n)$ represent the clean and estimated clean speech, respectively. The offset Δ_p accounts for the process delay of the noise reduction algorithm. However, the SNR measure has specific shortcomings where strong signal sections affect the measure more than weak signal sections [11]. The SNR_{SEG} , defined as

$$\text{SNR}_{\text{SEG}} = \frac{10}{P} \sum_p \log_{10} \frac{\sum_{n=0}^{N-1} |s(n + Np)|^2}{\sum_{n=0}^{N-1} |s(n + Np) - \hat{s}(n + Np + \Delta_p)|^2} \quad (\text{dB}), \quad (5.2)$$

averages the SNR of segments of length N samples long, usually around 16 ms. Since in the case of quantized signals $\sum_n |s(n)|^2$ or $\sum_n |s(n) - \hat{s}(n + \Delta_p)|^2$ can be zero over short sections, the following alternate form is used in the presented results. Using

$$\text{SNR}_{\text{SEG}} = 10 \log_{10} \left(10^{\sum_p \frac{SS(p)}{P}} - 1 \right) \quad (\text{dB}), \quad (5.3)$$

where

$$SS(p) = \log_{10} \left(1 + \frac{\sum_{n=0}^{N-1} |s(n + Np)|^2}{\eta + \sum_{n=0}^{N-1} |s(n + Np) - \hat{s}(n + Np + \Delta_p)|^2} \right), \quad (5.4)$$

η is a small value to prevent division by zero, and the addition of the unity term prevents a $\log(0)$ condition. Also, due to the addition of the unity term, segments with SNR below 0 dB are discounted. This results in a measure that balances the strong and weak sections of the signal.

The third basic noise measure used is the SNR_{IMPR} , which is used to evaluate the performance of noise suppression algorithms [8, 52]. It is given by the difference between

the input and output segmental SNR:

$$\text{SNR}_{\text{IMPR}} = \frac{1}{P} \sum_p 10 \log_{10} \frac{\sum_{n=0}^{N-1} |v(n + pN)|^2}{\sum_{n=0}^{N-1} |s(n + Np) - \hat{s}(n + Np + \Delta_p)|^2} \quad (\text{dB}), \quad (5.5)$$

where $v(n)$ is the background noise that was added to the clean speech signal (see Ch. 3).

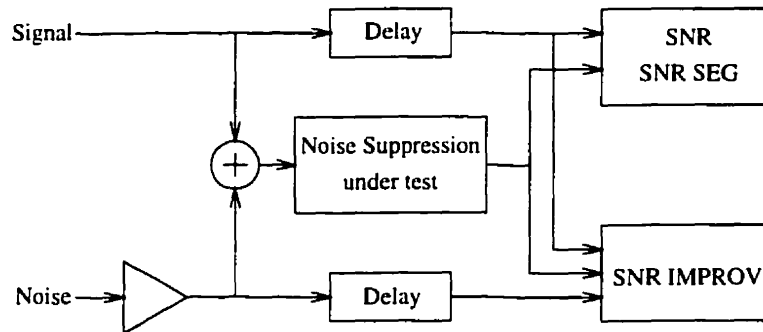


Fig. 5.1 Setup for obtaining SNR, SNR_{SEG} , and SNR_{IMPR} .

Figure 5.1 summarises the testing setup for the objective measurements. The noise, attenuated to achieve the desired initial SNR, is added to the signal, which is processed by the method being evaluated. The signal and noise are delayed to account for the process delay before being used to calculate the SNR, SNR_{SEG} , and SNR_{IMPR} .

Table 5.1 shows the results of objective measurements, sorted in descending order of SNR_{IMPR} , of the speech signal mixed with the vehicle interior noise at an initial SNR of 0 dB.

The data presented in Table 5.1 suggests that the proposed method (PNRF) performs well when evaluated by the SNR_{IMPR} and SNR measurements. Also, the ranking by these two measures is reasonably similar (in the plain SNR measure, the EVRC algorithm outperforms the audio enhancement method by Tsoukalas *et al*).

Perhaps most surprising is the result from the SNR_{SEG} measurement, which does not correlate well with the rankings of the other measures. This may be due to the higher emphasis on the signal sections with low energy. As implemented, most noise reduction methods leave significant amounts of residual noise to ‘hide’ artifacts (see Sec. 4.3.4).

Table 5.1 Objective measurement results with 0 dB initial SNR

Method	SNR_{IMPR}	SNR	SNR_{SEG}
Tsoukalas (Speech)	14.45	9.27	1.64
PNRF	12.98	6.94	0.161
Tsoukalas (Audio)	10.54	5.78	1.40
EVRC	8.81	6.25	-0.101
Virag	8.24	4.18	1.56
Boll	7.26	3.84	0.672
Haulick	7.25	3.84	0.662

The next table, Table 5.2 shows the results obtained using an initial SNR of 6 dB (vehicle interior noise). Again, the table is sorted by the SNR_{IMPR} result.

Table 5.2 Objective measurement results with 6 dB initial SNR

Method	SNR_{IMPR}	SNR	SNR_{SEG}
Tsoukalas (Speech)	12.93	12.52	4.02
PNRF	11.28	10.27	2.44
Tsoukalas (Audio)	9.46	10.88	4.01
Virag	7.85	9.99	4.49
EVRC	7.82	10.62	2.55
Boll	6.85	9.55	3.74
Haulick	6.83	9.54	3.72

As in Table 5.1, the SNR_{IMPR} and SNR measurements correlate well, and suggest that the PNRF performs well ahead of some of the older methods. Comparing Table 5.1 to Table 5.2, it is notable that both the SNR and SNR_{SEG} measurements increased significantly, and (as can be expected) that the SNR_{IMPR} decreased slightly. These differences can be explained by the fact that all the algorithms attempt to only reduce the noise to acceptable levels, rather than removing the noise completely. Thus, with a higher initial SNR, the amount of processing is reduced, reducing the SNR_{IMPR} while increasing the SNR and SNR_{SEG} measurements.

5.3 Subjective Comparisons

Since the intent of the noise suppression schemes presented is to improve the perceived quality of a signal, subjective evaluation by human listeners is not just essential, but key to evaluating the proposed method. The methods for *formal* subjective testing are rigidly specified; most common in the telecommunications field is *Mean Opinion Score* (MOS) testing, as specified by the ITU-T recommendations P.80 [53] and P.830 [54].

In the subjective testing for this thesis, a simpler A-B comparison was used. In this test, each subject is presented with two results from noise suppression algorithms, and has to indicate whether the first or the second result is preferred¹.

The A-B test was prepared by first creating n results to be compared to each other. These results were combined by creating testfiles consisting of two results separated by a 1 s pause. Thus $n^2 - n$ testfiles are created consisting of all possible combinations, in both presentation orders, of different results. However, this results in a large number of testfiles if n is large.

To reduce the number of test pairs, two of the methods were excluded after informal listening tests. The method proposed by Haulick *et al* was excluded because it provided little additional processing when compared to Boll's method. This is clearly visible from the objective results above. In addition the difference between the signal processed by Boll's and Haulick's method was found to be in the order of 40 dB SNR_{SEG}. Thus, only Boll's method was included in the test suite, to act as a baseline reference.

Also excluded from the test suite was Tsoukalas' method for audio signal enhancement. In initial testing it was decided that the amount of musical noise produced by this method was very strong and disturbing².

However, one additional comparison file was included to verify that processing provided an *overall* improvement. This additional file consisted of the unprocessed speech file with 3 dB (labeled *Ref+3 dB*) less noise than the original noisy file.

Subjects found even the reduced set (30 testfiles) to be quite tedious to evaluate. No specific listening instructions were given, though two or three randomly selected test pairs were played to the subject before the responses were recorded, to avoid a shift in focus

¹A "No Preference" response was allowed

²One subject referred to the musical noise as "bathroom noise." Musical noise created by algorithms incorporating a perceptual model has a very different character than musical noise created by an algorithm operating in linear frequency domain.

while familiarizing the subject with the testing procedure.

The sound was reproduced on a pair of self-powered loudspeakers typical for a computer workstation. The subjects were free to adjust the volume to their liking. Playback was directly from a 16-bit linear encoded sound file to the speakers. The listening test was performed in a small office with some ambient noise, mostly due to the computer workstation. This setup was chosen to represent a typical speech playback situation.

The following data was obtained by presenting 12 subjects with the processed speech files as described. However, given the duration of each test, not all the subjects participated in both tests. The subjects were students aged 21 to 28 and mostly from within the engineering faculty.

In the first test (speech with vehicle noise added at 0 dB) a total of 9 subjects (5 male and 4 female) participated. The results, shown in Table 5.3, give the percentage of responses in which the “compared” method was preferred over PNRF, the percentage for which PNRF was preferred over the compared method, and the percentage of responses indicating no preference.

Table 5.3 Subjective results for speech segments at 0 dB SNR

Test method	Test method preferred	PNRF preferred	<i>no decision</i>
Tsoukalas (Speech)	61%	33%	6%
EVRC	33%	61%	6%
<i>Ref</i> +3 dB	22%	72%	6%
Virag	6%	94%	0%
Boll	6%	94%	0%

The results presented in Table 5.3 show some agreement with the objective results in Table 5.1. Tsoukalas’ method for speech enhancement outperforms all other methods. However, given the small sample size (6% representing one response), the differences between Tsoukalas’ method, PNRF, and EVRC are too close to draw conclusions (Note that the comparison between Tsoukalas’ method and EVRC also yielded a preference for Tsoukalas’ of 61%, and a preference for EVRC of 33%).

The experiment was constructed to account for presentation bias, by presenting the processing results in both orders. At 0 dB SNR, a noticeable bias emerged towards the second sample played. When the combination Tsoukalas-PNRF was presented, 55% of re-

sponses were in favour of PNRF, versus 33% in favour of Tsoukalas. When the combination PNRF-Tsoukalas was presented, 88% of responses were in favour of Tsoukalas, versus 11% in favour of PNRF.

Also noteworthy is that based on comments by the subjects, the poor performance of Boll's and Virag's methods is mainly due to the musical noise. In the test, Virag's method was preferred over Boll's in 78% of the responses. Full results are tabulated in Appendix B.

The second test was performed using 8 subjects, 4 male and 4 female. The results for this test are shown in Table 5.4. As in the previous table, only the comparison with PNRF is shown, and sorted accordingly.

Table 5.4 Subjective results for speech segments at 6 dB SNR

Comparison method	Comparison preferred	PNRF preferred	<i>no decision</i>
Tsoukalas (Speech)	56%	38%	6%
EVRC	13%	81%	6%
<i>Ref</i> +3 dB	0%	100%	0%
Virag	0%	100%	0%
Boll	0%	100%	0%

Table 5.4 shows a clearer preference of PNRF over most of the other methods, again with the exception of Tsoukalas' method. More so than in the previous test, the preference of Tsoukalas' method over PNRF is too small to generalize this result. However, the preference of PNRF over EVRC is much more pronounced. The complete aggregate results can be found in Appendix B.

Overall, it was found that listeners quickly focused on the musical noise in the processed signal. When asked about the musical noise after the tests, most subjects cited it as the main factor in making a decision about which method was preferred. Some noted the distortion in the speech signal, but before being specifically asked about it, considered it a secondary factor in the overall quality of the signal. It can be argued that since during a single test the subject hears the same 4 sentences 60 times, the subject's focus quickly shifts from the actual speech to the background noise, which varies considerably between the individual noise reduction methods. This could explain the slight preference of Tsoukalas' speech enhancement method (which has considerable speech distortion, but almost no musical noise) over Soulodre's PNRF method which has some musical noise, but

little detectable distortion.

5.4 Summary

This chapter presented the results from both objective and subjective comparisons of the proposed noise reduction method with other speech enhancement methods. The proposed method, derived from Soulodre's method for removing camera noise from film soundtracks, is shown to perform well in comparison to most of the other methods discussed in the previous chapter. The only method consistently outperforming Soulodre's method in objective and subjective measurements is the speech enhancement method proposed by Tsoukalas *et al.*, which focuses on suppressing musical noise at the expense of signal distortion.

Chapter 6

Conclusion

In this thesis, the problem of acoustic noise suppression is explored, using properties of the human hearing system in an attempt to improve performance. It was shown that using masking properties of the hearing system allows for improved noise reduction. A novel method for noise reduction in speech signals has been proposed. This method was shown to outperform non-auditory based methods, and compared well with other perceptually motivated noise reduction methods. It was found that the proposed method, Soulodre's PNRF combined with the ITU's PEAQ auditory model, had more musical noise but less signal distortion than a method proposed by Tsoukalas *et al.* which obtained marginally better results in informal subjective testing.

6.1 Summary

The problem of noise reduction in speech signals and audio signals was introduced. Noise reduction is used in the telecommunication field to improve intelligibility or perceived quality of the signal. Another area where noise reduction is applied is in the process of audio archive restoration. These different fields have distinct requirements, that cannot always be simultaneously satisfied, and thus various methods for noise reduction have been developed. Widely used in the problem of noise reduction in speech signals are methods based on the processing of short-time spectral amplitudes. These methods have been further improved by using an auditory model to reduce the amount of processing applied to the signal while maintaining the perceived level of noise suppression.

Chapter 2 presents an overview of the human hearing system. The human auditory

system converts sound waves into signals that are received by the brain. The acoustic signal is transformed into a displacement of the basilar membrane, which causes nerve cells to react. Nonlinearities in this system, such as interaction between nerve cells and the behavior of the basilar membrane, give rise to masking effects. These masking effects cause some sounds to be inaudible in the presence of other sounds. Auditory models are used to predict these masking effects.

In Chapter 3 some non-auditory noise reduction methods are introduced. Spectral subtraction is a common method, and is based on modifying the short-time spectral shape of the signal. It is assumed that the spectrum of the noise is relatively stationary, and that the power spectra of the clean signal and the noise are additive. However, spectral subtraction and related methods create artifacts in the estimated signal, such as musical noise and distortion. These artifacts are disturbing to the listener, and should be avoided. Other methods for noise reduction have been developed that attempt to increase performance to reduce residual noise, musical noise, and signal distortion.

Models for estimating the masking threshold and their application in noise reduction methods are described in Chapter 4. Different auditory models were developed for speech coding methods, audio coding methods, objective perceptual quality measures, and noise reduction. These models are used in noise reduction methods to iteratively estimate the clean signal, estimate the clean signal psychoacoustic representation, or identify audible musical noise. A novel noise reduction method is proposed, based on an auditory model from a standardized perceptual quality assessment method, and a noise reduction rule designed to remove a specific type of noise from audio signals. For comparison, other perceptual noise reduction methods have been implemented using the same auditory model.

An evaluation of the proposed method (PNRF), and a comparison with the other methods is presented in Chapter 5. Objective and informal subjective results show that the PNRF compares favorably to other perceptual noise reduction methods. Only one method, exhibiting less musical noise at the expense of higher signal distortion, is rated as being slightly better in the objective and subjective results.

6.2 Future Research Directions

Many issues are unresolved in the problem of noise reduction. The noise reduction method presented in this thesis shows that effective noise reduction with little or no perceivable

distortion is attainable. This section addresses some issues that may further improve the performance of the proposed method, and areas other than narrowband speech enhancement where the PNRF could be effectively applied as well.

6.2.1 Iterative clean speech estimation

In the objective and subjective results presented in Chapter 5, Tsoukalas' method outperforms PNRF by fairly small margins. The good performance of Tsoukalas' method may in part be attributed to its iterative nature. Using the result of one iteration of the noise reduction process as estimate of the clean speech signal for the next, the clean speech estimate is successively improved. A similar approach can be used with the PNRF, since it uses an initial clean speech estimate based simply on Boll's method. Since PNRF achieves good results with only one iteration, a much smaller number of iterations than used by Tsoukalas' method would be necessary to match results with Tsoukalas' method.

6.2.2 Soft-decision VAD

As mentioned in Chapter 5, test subjects focused on the musical noise that was audible in the speech pauses of the processed signal. Since for the noise estimation it is necessary to identify the active speech segments using a Voice Activity Detector, this information may be used to modify the parameters of the algorithm dynamically. Care should be taken to avoid sudden changes, which would sound unnatural. One method to work around this problem would be to use a VAD that provides more information than a simple speech/silence decision. What kind of information a VAD should generate and how this would be used by the algorithm are issues that need to be addressed.

6.2.3 Application to wide-band signals

While briefly discussing the applications of noise reduction in other areas, the focus of this thesis has mainly been on the enhancement of speech signal sampled at telephone bandwidth. However, since both the suppression rule and the auditory model were originally developed for use in wideband (48000 Hz sampling rate) systems, the PNRF should be applicable equally well to wideband speech (typically sampled at 16000 Hz) and audio signal enhancement. The biggest obstacle in the latter application is reliable signal/silence detection, to obtain a good noise spectrum estimate.

6.2.4 Lower complexity masking model

The evaluation of auditory models and noise suppression algorithms in this thesis was focused primarily on performance. The issue of computational complexity has been mentioned only briefly. However, in a practical setting, this issue can be very important if the processing must be performed on a portable device, or on a fixed device that processes several hundred channels independently. Thus, reducing the complexity of the algorithm or the model can reduce the cost to the end-user.

One target for optimization would be the nonlinear normalized summation step of the PEAQ model. This step was found to be one of the slowest parts of the masking threshold calculation. It would be worth investigating if this step can be simplified without affecting the performance of the overall noise suppression algorithm.

Appendix A

Frequency bands for PEAQ

Group	Lower Freq.	Centre Freq.	Upper Freq.	Freq. Width
0	80.000	91.708	103.445	23.445
1	103.445	115.216	127.023	23.577
2	127.023	138.870	150.762	23.739
3	150.762	162.702	174.694	23.932
4	174.694	186.742	198.849	24.155
5	198.849	211.019	223.257	24.408
6	223.257	235.566	247.950	24.693
7	247.950	260.413	272.959	25.009
8	272.959	285.593	298.317	25.358
9	298.317	311.136	324.055	25.738
10	324.055	337.077	350.207	26.151
11	350.207	363.448	376.805	26.598
12	376.805	390.282	403.884	27.079
13	403.884	417.614	431.478	27.594
14	431.478	445.479	459.622	28.145
15	459.622	473.912	488.353	28.731
16	488.353	502.950	517.707	29.354
17	517.707	532.629	547.721	30.014

continued on next page

Group	Lower Freq.	Centre Freq.	Upper Freq.	Freq. Width
18	547.721	562.988	578.434	30.713
19	578.434	594.065	609.885	31.451
20	609.885	625.899	642.114	32.229
21	642.114	658.533	675.161	33.048
22	675.161	692.006	709.071	33.909
23	709.071	726.362	743.884	34.814
24	743.884	761.644	779.647	35.763
25	779.647	797.898	816.404	36.757
26	816.404	835.170	854.203	37.799
27	854.203	873.508	893.091	38.888
28	893.091	912.959	933.119	40.028
29	933.119	953.576	974.336	41.218
30	974.336	995.408	1016.797	42.461
31	1016.797	1038.511	1060.555	43.758
32	1060.555	1082.938	1105.666	45.111
33	1105.666	1128.746	1152.187	46.521
34	1152.187	1175.995	1200.178	47.991
35	1200.178	1224.744	1249.700	49.522
36	1249.700	1275.055	1300.816	51.116
37	1300.816	1326.992	1353.592	52.776
38	1353.592	1380.623	1408.094	54.502
39	1408.094	1436.014	1464.392	56.298
40	1464.392	1493.237	1522.559	58.167
41	1522.559	1552.366	1582.668	60.109
42	1582.668	1613.474	1644.795	62.128
43	1644.795	1676.641	1709.021	64.226
44	1709.021	1741.946	1775.427	66.406
45	1775.427	1809.474	1844.098	68.671
46	1844.098	1879.310	1915.121	71.023

continued on next page

Group	Lower Freq.	Centre Freq.	Upper Freq.	Freq. Width
47	1915.121	1951.543	1988.587	73.466
48	1988.587	2026.266	2064.590	76.003
49	2064.590	2103.573	2143.227	78.637
50	2143.227	2183.564	2224.597	81.371
51	2224.597	2266.340	2308.806	84.208
52	2308.806	2352.008	2395.959	87.154
53	2395.959	2440.675	2486.169	90.210
54	2486.169	2532.456	2579.551	93.382
55	2579.551	2627.468	2676.223	96.672
56	2676.223	2725.832	2776.309	100.086
57	2776.309	2827.672	2879.937	103.627
58	2879.937	2933.120	2987.238	107.302
59	2987.238	3042.309	3098.350	111.112
60	3098.350	3155.379	3213.415	115.065
61	3213.415	3272.475	3332.579	119.164
62	3332.579	3393.745	3455.993	123.415
63	3455.993	3519.344	3583.817	127.823
64	3583.817	3649.432	3716.212	132.395
65	3716.212	3784.176	3853.348	137.136
66	3853.348	3923.748	3995.399	142.051
67	3995.399	4068.324	4142.547	147.148
68	4142.547	4218.090	4294.979	152.432
69	4294.979	4373.237	4452.890	157.911
70	4452.890	4533.963	4616.482	163.592
71	4616.482	4700.473	4785.962	169.480
72	4785.962	4872.978	4961.548	175.585
73	4961.548	5051.700	5143.463	181.915
74	5143.463	5236.866	5331.939	188.476
75	5331.939	5428.712	5527.217	195.278

continued on next page

Group	Lower Freq.	Centre Freq.	Upper Freq.	Freq. Width
76	5527.217	5627.484	5729.545	202.329
77	5729.545	5833.434	5939.183	209.637
78	5939.183	6046.825	6156.396	217.214
79	6156.396	6267.931	6381.463	225.067
80	6381.463	6497.031	6614.671	233.208
81	6614.671	6734.420	6856.316	241.646
82	6856.316	6980.399	7106.708	250.392
83	7106.708	7235.284	7366.166	259.458
84	7366.166	7499.397	7635.020	268.854
85	7635.020	7773.077	7913.614	278.594
86	7913.614	8056.673	8202.302	288.688
87	8202.302	8350.547	8501.454	299.152
88	8501.454	8655.072	8811.450	309.996
89	8811.450	8970.639	9132.688	321.237
90	9132.688	9297.648	9465.574	332.887
91	9465.574	9636.520	9810.536	344.962
92	9810.536	9987.683	10168.013	357.477
93	10168.013	10351.586	10538.460	370.447
94	10538.460	10728.695	10922.351	383.891
95	10922.351	11119.490	11320.175	397.824
96	11320.175	11524.470	11732.438	412.264
97	11732.438	11944.149	12159.670	427.231
98	12159.670	12379.066	12602.412	442.742
99	12602.412	12829.775	13061.229	458.817
100	13061.229	13296.850	13536.710	475.480
101	13536.710	13780.887	14029.458	492.748
102	14029.458	14282.503	14540.103	510.645
103	14540.103	14802.338	15069.295	529.192
104	15069.295	15341.057	15617.710	548.415

continued on next page

Group	Lower Freq.	Centre Freq.	Upper Freq.	Freq. Width
105	15617.710	15899.345	16186.049	568.339
106	16186.049	16477.914	16775.035	588.986
107	16775.035	17077.504	17385.420	610.385
108	17385.420	17690.045	18000.000	614.580

Appendix B

Subjective testing results

Table B.1 Number of answers indicating preference of "A" at 0 dB initial SNR

A	B					
	Tsoukalas	PNRF	EVRC	Ref+3dB	Virag	Boll
Tsoukalas		3	5	8	8	8
PNRF	1		4	6	9	8
EVRC	3	2		5	8	7
Ref+3dB	1	2	2		6	8
Virag	0	1	2	2		7
Boll	0	0	1	1	2	

Table B.2 Number of answers indicating preference of "B" at 0 dB initial SNR

A	B					
	Tsoukalas	PNRF	EVRC	Ref+3dB	Virag	Boll
Tsoukalas		5	3	1	1	1
PNRF	8		4	2	0	1
EVRC	6	7		4	1	2
Ref+3dB	8	7	7		2	0
Virag	9	8	7	6		2
Boll	9	9	8	7	7	

Table B.3 Number of answers indicating preference of "A" at 6 dB initial SNR

A	B					
	Tsoukalas	PNRF	EVRC	Ref+3dB	Virag	Boll
Tsoukalas		5	8	7	8	8
PNRF	2		7	8	8	8
EVRC	3	2		7	8	8
Ref+3dB	1	0	3		6	8
Virag	0	0	1	3		4
Boll	0	0	0	1	1	

Table B.4 Number of answers indicating preference of "B" at 6 dB initial SNR

A	B					
	Tsoukalas	PNRF	EVRC	Ref+3dB	Virag	Boll
Tsoukalas		2	0	1	0	0
PNRF	5		0	0	0	0
EVRC	5	6		1	0	0
Ref+3dB	7	8	5		1	0
Virag	8	8	6	4		3
Boll	8	8	8	6	7	

References

- [1] S. V. Vaseghi, *Advanced Signal Processing and Digital Noise Reduction*. Wiley Teubner, 1996.
- [2] S. J. Godsill and P. J. W. Rayner, *Digital Audio Restoration*. Springer Verlag, 1998.
- [3] J. John R. Deller, J. H. L. Hansen, and J. G. Proakis, *Discrete-Time Processing of Speech Signals*. New York: IEEE Press, 2000.
- [4] G. Soulodre, *Adaptive Methods for Removing Camera Noise from Film Soundtracks*. PhD thesis, McGill University, Montréal, Canada. 1998.
- [5] T. Painter and A. Spanias, "Perceptual coding of digital audio." *Proc. IEEE*, vol. 88, pp. 451–513, Apr. 2000.
- [6] D. E. Tsoukalas, J. N. Mourjopoulos, and G. Kokkinakis, "Speech enhancement based on audible noise suppression," *IEEE Trans. Speech and Audio Processing*, vol. 5, pp. 497–514, Nov. 1997.
- [7] D. E. Tsoukalas, J. N. Mourjopoulos, and G. Kokkinakis, "Perceptual filters for audio signal enhancement," *J. Audio Eng. Soc.*, vol. 45, pp. 22–35, Jan/Feb 1997.
- [8] N. Virag, "Single channel speech enhancement based on masking properties of the human auditory system," *IEEE Trans. Speech and Audio Processing*, vol. 7, pp. 126–137, Mar. 1999.
- [9] T. Haulick, K. Linhard, and P. Schrögmeier, "Residual noise suppression using psychoacoustic criteria," in *Eurospeech 97*, (Rhodes, Greece), pp. 1395–1398, Sept. 1997.
- [10] E. Zwicker and H. Fastl, *Psychoacoustics*. Springer Verlag, 2nd ed., 1999.
- [11] D. O'Shaughnessy, *Speech Communications: Human and Machine*. IEEE Press, 2nd ed., 2000.
- [12] B. Gold and N. Morgan, *Speech and Audio Signal Processing: Processing and Perception of Speech and Music*. John Wiley & Sons. 1999.

- [13] B. C. J. Moore, *An Introduction to the Psychology of Hearing*. Academic Press, 4th ed., 1997.
- [14] E. Terhardt, G. Stoll, and M. Seewann, "Algorithm for extraction of pitch and pitch salience from complex tonal signals," *J. Acoust. Soc. Am.*, vol. 71, Mar. 1982.
- [15] W. M. Hartmann. *Signals, Sound, and Sensation*. Springer Verlag, 1997.
- [16] T. Thiede, W. C. Treurniet, R. Bitto, C. Schmidner, T. Sporer, J. G. Beerends, C. Colomes, M. Keyhl, G. Stoll, K. Brandenburg, and B. Feiten. "PEAQ - the ITU standard for objective measurement of perceived audio quality," *J. Audio Eng. Soc.*, vol. 48, Jan. 2000.
- [17] E. Zwicker and E. Terhardt, "Analytical expressions for critical-band rate and critical bandwidth as a function of frequency," *J. Acoust. Soc. Am.*, vol. 68, Nov. 1980.
- [18] S. Voran. "Observations on auditory excitation and masking patterns," in *Applications of Signal Processing to Audio and Acoustics, IEEE ASSP Workshop on*, pp. 206–209, Oct. 1995.
- [19] S. F. Boll, "Suppression of acoustic noise in speech using spectral subtraction," *IEEE Trans. Acoustics, Speech, Signal Processing*, vol. ASSP-27, Apr. 1979.
- [20] S. F. Boll, "A spectral subtraction algorithm for suppression of acoustic noise in speech," in *Proc. IEEE Int. Conf. on Acoustics, Speech, Signal Processing*, (Washington, DC), pp. 200–203, Apr. 1979.
- [21] R. J. McAulay and M. L. Malpass, "Speech enhancement using a soft-decision noise suppression filter," *IEEE Trans. Acoustics, Speech, Signal Processing*, vol. ASSP-28, Apr. 1980.
- [22] J. S. Lim and A. V. Oppenheim, "Enhancement and bandwidth compression of noisy speech," *Proc. IEEE*, vol. 67, Dec. 1979.
- [23] A. S. Spanias, "Speech coding: A tutorial review," *Proc. IEEE*, vol. 82, pp. 1541–1582, Oct. 1994.
- [24] M. Berouti, R. Schwartz, and J. Makhoul, "Enhancement of speech corrupted by acoustic noise," in *Proc. IEEE Int. Conf. on Acoustics, Speech, Signal Processing*, (Washington, DC), pp. 208–211, Apr. 1979.
- [25] R. E. Crochiere. "A weighted overlap-add method of short-time fourier analysis/synthesis," *IEEE Trans. Acoustics, Speech, Signal Processing*, vol. 28, Feb. 1980.

- [26] J. G. Proakis and D. G. Manolakis, *Digital Signal Processing: Principles, Algorithms and Applications*. Prentice-Hall, 3rd ed., 1996.
- [27] A. V. Oppenheim and R. W. Schaffer, *Discrete-time Signal Processing*. Prentice-Hall, 1989.
- [28] "Enhanced variable rate codec, speech service option 3 for wideband spread spectrum digital systems," Jan. 1996. TR-45, PN-3292 (to be published as IS-127).
- [29] "Digital cellular telecommunications system (Phase 2+); Voice Activity Detector (VAD) for Adaptive Multi-Rate (AMR) speech traffic channels; General description (GSM 06.94 version 7.1.0 Release 1998)," 1998.
- [30] Y. Ephraim and D. Mahlah, "Speech enhancement using a minimum mean-square error short-time spectral amplitude estimator," *IEEE Trans. Acoustics, Speech, Signal Processing*, vol. 32, pp. 1109–1121, Dec. 1984.
- [31] O. Cappé, "Elimination of the musical noise phenomenon with the Ephraim and Malah noise suppressor," *IEEE Trans. Speech and Audio Processing*, vol. 2, pp. 345–349, Apr. 1994.
- [32] P. Scalart and J. V. Filho, "Speech enhancement based on a priori signal to noise estimation," in *Proc. IEEE Int. Conf. on Acoustics, Speech, Signal Processing*, (Atlanta, GA), pp. 629–632, May 1996.
- [33] H. Gustafsson, S. Nordholm, and I. Claesson, "Spectral subtraction with adaptive averaging of the gain function," in *Eurospeech 99*, (Budapest, Hungary), pp. 2599–2602, Sept. 1999.
- [34] Y. Ephraim and H. L. Van Trees, "A signal subspace approach for speech enhancement," *IEEE Trans. Speech and Audio Processing*, vol. 3, July 1995.
- [35] M. C. Reccione, "The enhanced variable rate coder: Toll quality speech for CDMA," *Int. J. of Speech Technology*, pp. 305–315, 1999.
- [36] J. D. Johnston, "Transform coding of audio signals using perceptual noise criteria," *IEEE J. Selected Areas in Comm.*, vol. 6, pp. 314–323, Feb. 1988.
- [37] M. R. Schroeder, B. S. Atal, and J. L. Hall, "Optimizing digital speech coders by exploiting masking properties of the human ear," *J. Acoust. Soc. Am.*, vol. 66, Dec. 1979.
- [38] D. Sinha and A. H. Tewfik, "Low bit rate transparent audio compression using adapted wavelets," *IEEE Trans. Signal Processing*, vol. 41, pp. 3463–3479, Dec. 1993.

- [39] J. G. Beerends and J. A. Stemerdink, "A perceptual audio quality measure based on a psychoacoustic sound representation," *J. Audio Eng. Soc.*, vol. 40, Dec. 1992.
- [40] "Method for objective measurements of perceived audio quality," 1998. Recommendation ITU-R BS.1387.
- [41] W. C. Treurniet and G. Soulodre, "Evaluation of the ITU-R objective audio quality measurement method," *J. Audio Eng. Soc.*, vol. 48, Mar. 2000.
- [42] T. L. Petersen and S. F. Boll, "Acoustic noise suppression in the context of a perceptual model," in *Proc. IEEE Int. Conf. on Acoustics, Speech, Signal Processing*, (Atlanta, Georgia), pp. 1086–1088, Apr. 1981.
- [43] Y. M. Cheng and D. O'Shaughnessy, "Speech enhancement based conceptually on auditory evidence," *IEEE Trans. Signal Processing*, vol. 39, Sept. 1991.
- [44] D. Tsoukalas, M. Paraskevas, and J. Mourjopoulos, "Speech enhancement using psychoacoustic criteria," in *Proc. IEEE Int. Conf. on Acoustics, Speech, Signal Processing*, (Minneapolis, MN), pp. II-359–II-362, Apr. 1993.
- [45] T. E. Eger, J. C. Su, and L. W. Varner, "A nonlinear spectrum processing technique for speech enhancement," in *Proc. IEEE Int. Conf. on Acoustics, Speech, Signal Processing*, (San Diego, CA), pp. 18A.1.1–18A.1.4, Mar. 1984.
- [46] P. M. Clarkson and S. F. Bahgat, "Envelope expansion methods for speech enhancement," *J. Acoust. Soc. Am.*, vol. 89, pp. 1378–1382, Mar. 1991.
- [47] M. Lorber and R. Hoeldrich, "A combined approach for broadband noise reduction," in *Proc. IEEE Workshop on Audio and Acoustics*, (Mohonk, NY), Oct. 1997.
- [48] "Signal Processing Information Base." Located at <http://spib.rice.edu/spib.html>, URL current as of March 2001.
- [49] "Digital cellular telecommunication system (phase 2+); results of the AMR noise suppression selection phase," June 2000. GSM 06.78 version 0.5.0.
- [50] "Objective measurement of active speech level." 1993. Recommendation ITU-T P.56.
- [51] S. R. Quackenbush, T. P. Barnwell III, and M. A. Clements, *Objective Measures of Speech Quality*. Prentice-Hall, 1988.
- [52] "Digital cellular telecommunications system (Phase 2+); Minimum Performance Requirements for Noise Suppressor; Application to the AMR Speech Encoder (GSM 06.77 version 1.3.0)," 2000.

- [53] "Methods for subjective determination of transmission quality," 1993. Recommendation ITU-T P.80.
- [54] "Method for objective and subjective assessment of telephone-band and wideband digital codecs," 1996. Recommendation ITU-T P.830.